IL-1R–MyD88 signaling in keratinocyte transformation and carcinogenesis

Christophe Cataisson,[1] Rosalba Salcedo,[4] Shakeeb Hakim,[1] B. Andrea Moffitt,[1] Lisa Wright,[1] Ming Yi,[3] Robert Stephens,[3] Ren-Ming Dai,[2,4] Lyudmila Lyakh,[2] Dominik Schenten,[5,6] H. Stuart Yuspa,[1] and Giorgio Trinchieri[2]

[1]Laboratory of Cancer Biology and Genetics and [2]Cancer and Inflammation Program, National Cancer Institute, Bethesda, MD 20892
[3]Advanced Biomedical Computing Center, Information Systems Program, [4]SAIC-Frederick Inc., Frederick, MD 21701
[5]Department of Immunobiology and [6]Howard Hughes Medical Institute, Yale University School of Medicine, New Haven, CT 06510

Constitutively active RAS plays a central role in the development of human cancer and is sufficient to induce tumors in two-stage skin carcinogenesis. RAS-mediated tumor formation is commonly associated with up-regulation of cytokines and chemokines that mediate an inflammatory response considered relevant to oncogenesis. In this study, we report that mice lacking IL-1R or MyD88 are less sensitive to topical skin carcinogenesis than their respective wild-type (WT) controls. MyD88$^{-/-}$ or IL-1R$^{-/-}$ keratinocytes expressing oncogenic RAS are hyperproliferative and fail to up-regulate proinflammatory genes or down-regulate differentiation markers characteristic of RAS-expressing WT keratinocytes. Although RAS-expressing MyD88$^{-/-}$ keratinocytes form only a few small tumors in orthotopic grafts, IL-1R–deficient RAS-expressing keratinocytes retain the ability to form tumors in orthotopic grafts. Using both genetic and pharmacological approaches, we find that the differentiation and proinflammatory effects of oncogenic RAS in keratinocytes require the establishment of an autocrine loop through IL-1α, IL-1R, and MyD88 leading to phosphorylation of IκBα and NF-κB activation. Blocking IL-1α–mediated NF-κB activation in RAS-expressing WT keratinocytes reverses the differentiation defect and inhibits proinflammatory gene expression. Collectively, these results demonstrate that MyD88 exerts a cell-intrinsic function in RAS-mediated transformation of keratinocytes.

CORRESPONDENCE
H. Stuart Yuspa:
yuspas@mail.nih.gov
OR
Giorgio Trinchieri:
trinchig@mail.nih.gov

Abbreviations used: DMBA, 7,12-dimethylbenz[a]anthracene; EGFR, epidermal growth factor receptor; mRNA, messenger RNA; SCC, squamous cell carcinoma; TPA, 12-0-tetradecanoylphorbol-13-acetate.

Skin tumors are the most common form of cancer in the Caucasian population. Approximately 80% of nonmelanoma skin cancers are basal cell carcinomas, and 20% are squamous cell carcinomas (SCCs). Unlike most basal cell carcinomas, cutaneous SCCs are associated with risk of metastasis particularly in immunosuppressed patients (Brantsch et al., 2008). The multistage induction of squamous cell cancer on mouse skin as a consequence of chemical exposures has remarkable phenotypic and genotypic homology to human SCC development. Genetically altered mouse models have been instrumental in defining the respective contribution of signaling pathways on the development of SCCs in vivo. Central to the skin carcinogenesis process is the activation of the EGFR (epidermal growth factor receptor)–RAS–MAPK (mitogen-activated protein kinase) pathway in incipient tumor cells and the associated inflammatory process that appears to enhance tumor growth (Mueller, 2006). The molecular links and pathways bridging inflammation and cancer are being clarified with cytokine/chemokines and myeloid cells taking center stage (Porta et al., 2009). Among the transcription factors regulating cytokine/chemokine expression, NF-κB has been causally implicated with cancer-associated inflammation (Van Waes, 2007; Naugler and Karin, 2008). In addition to its proinflammatory activity, NF-κB has both antiapoptotic activities and can promote cell cycle progression, making its constitutive activation advantageous to cancer cells. In the skin, the innate immune system is a potent activator of NF-κB. Ligands of the Toll-like receptor/IL-1 receptor superfamily induce the recruitment of MyD88 (Myeloid differentiation primary response gene 88),

C. Cataisson and R. Salcedo contributed equally to this paper.

The Rockefeller University Press $30.00
J. Exp. Med. 2012 Vol. 209 No. 9 1689-1702
www.jem.org/cgi/doi/10.1084/jem.20101355

The Journal of Experimental Medicine

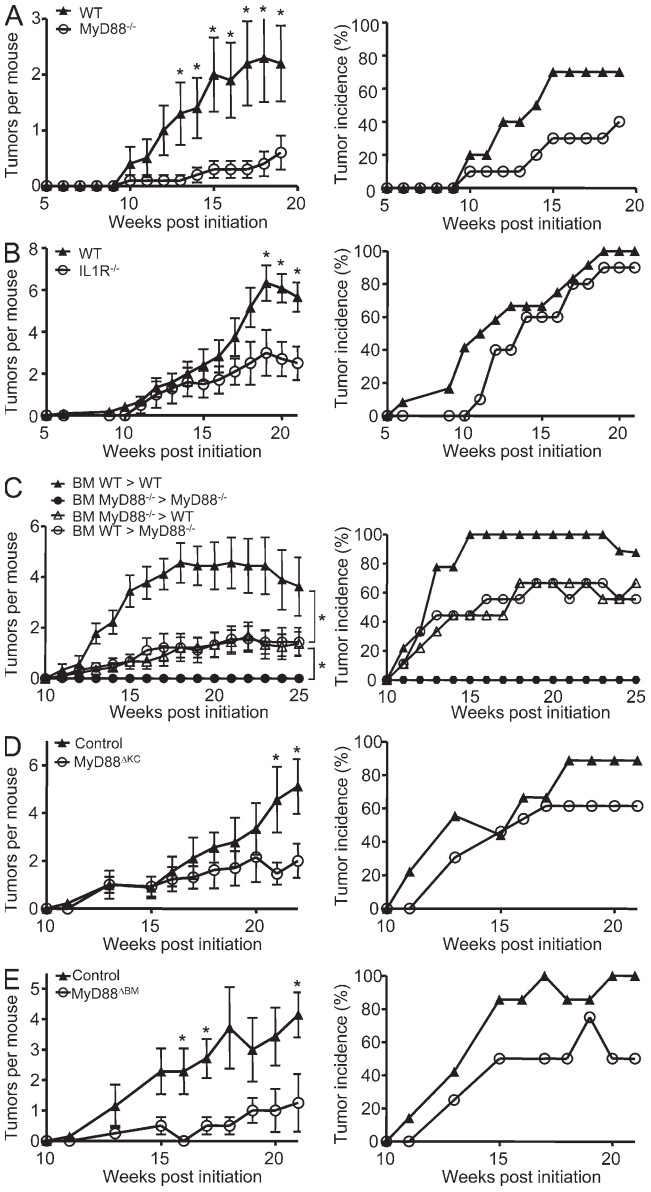

Figure 1. Responsiveness of MyD88$^{-/-}$, IL-1R$^{-/-}$, MyD88$^{-/-}$ BM chimeric, tissue-targeted MyD88-deficient mice, and their respective controls to chemically induced skin carcinogenesis. (A–E) Left panels represent the mean number of skin tumors per mouse (mean ± SEM). Right panels represent the percentage of mice with skin tumors. Mice were treated with DMBA/0.2 ml acetone at time 0 then with 10 nmol TPA/0.2 ml acetone three times a week for up to 20 wk. Papilloma development was monitored during the course of the experiment. (A) WT (n = 10) and MyD88$^{-/-}$ (n = 10). (B) WT (n = 12) and IL-1R$^{-/-}$ (n = 10). (C) Mice were lethally irradiated and 2 h later injected i.v. with 20 × 10^6 BM cells. 8 wk later, BM WT > WT (n = 9), BM MyD88$^{-/-}$ > MyD88$^{-/-}$ (n = 5), BM MyD88$^{-/-}$ > WT (n = 9), and BM WT > MyD88$^{-/-}$ (n = 9) groups were treated as in A, and papilloma development was followed during 25 wk. (D) MyD88$^{\Delta KC}$ (n = 13) and control littermates (n = 9). (E) MyD88$^{\Delta BM}$ (n = 4) and control littermates (n = 7). Data shown in A, B, and E are representative of three independent experiments, whereas data shown in C and D are representative of two independent experiments. Significant differences in the number of papillomas that develop at each time point were found by Student's t test (*, P < 0.05). In C, comparisons of BM WT > WT and BM MyD88$^{-/-}$ > WT (*, P < 0.05) and BM MyD88$^{-/-}$ > MyD88$^{-/-}$ and BM WT >MyD88$^{-/-}$ (*, P < 0.05) were analyzed by Mann-Whitney U test.

TRAF6, and protein kinases, including IRAK and IKK, ultimately leading to NF-κB activation (Dinarello, 2009). Activated keratinocytes are a potent source of IL-1α and IL-1β activity upon 12-0-tetradecanoylphorbol-13-acetate (TPA) or UV challenge (Kupper et al., 1986; Feldmeyer et al., 2007). Although IL-1 expression has been reported to enhance tumor invasiveness/metastasis and cellular interactions in the tumor microenvironment, less is known about its potential autocrine and paracrine function in the early stage of carcinogenesis (Apte et al., 2006). The mouse skin carcinogenesis model is particularly suited to explore pathways involved in early tumor formation because a single activated oncogene, H- or K-RAS, is sufficient to fully initiate keratinocytes. The clonal expansion of these cells into a squamous papilloma reveals the phenotype of initiated cells (RAS-keratinocytes). The current study defines an essential contribution of the IL-1R for the initiation of keratinocytes in vitro and MyD88 for papilloma formation after RAS activation. We uncover an obligatory role for autocrine IL-1α for the maintenance of NF-κB activity and induction of cytokines and chemokines in RAS-keratinocytes. We also report a previously unrecognized causal role of IL-1α and NF-κB in producing the altered differentiation phenotype exhibited by initiated keratinocytes.

RESULTS

MyD88 is required for 7,12-dimethylbenz[a]anthracene (DMBA)–TPA-induced skin carcinogenesis

MyD88$^{-/-}$ mice, IL-1R$^{-/-}$ mice, and their WT respective controls were compared for susceptibility to 400 nmol DMBA initiation followed by 10 nmol TPA three times a week for 20 wk of promotion. As previously described (Swann et al., 2008; Coste et al., 2010; Mittal et al., 2010), less than half of the MyD88-deficient mice on a C57BL/6NCr background developed skin papillomas after 4 mo, and those that developed tumors rarely developed more than one tumor, whereas the corresponding genetically matched WT controls developed the expected number for this strain (Fig. 1 A). An intermediate tumor burden developed in the more susceptible C57BL/6J background IL-1R$^{-/-}$ mice with ∼50% decrease in the number of papillomas per mouse in comparison with genetically matched controls (Fig. 1 B), suggesting that IL-1R may contribute a significant share of the signal going through MyD88 (Coste et al., 2010). However, unlike the MyD88-deficient mice, nearly 100% of IL-1R$^{-/-}$ developed at least one or more tumors, indicating that genetic background or additional factors contribute to the low tumor yield in MyD88-deficient mice. To address the cell population responsible for the skin carcinogenesis resistance observed in MyD88$^{-/-}$ mice, BM chimeras were generated by injecting MyD88$^{-/-}$ or WT BM cells into lethally irradiated

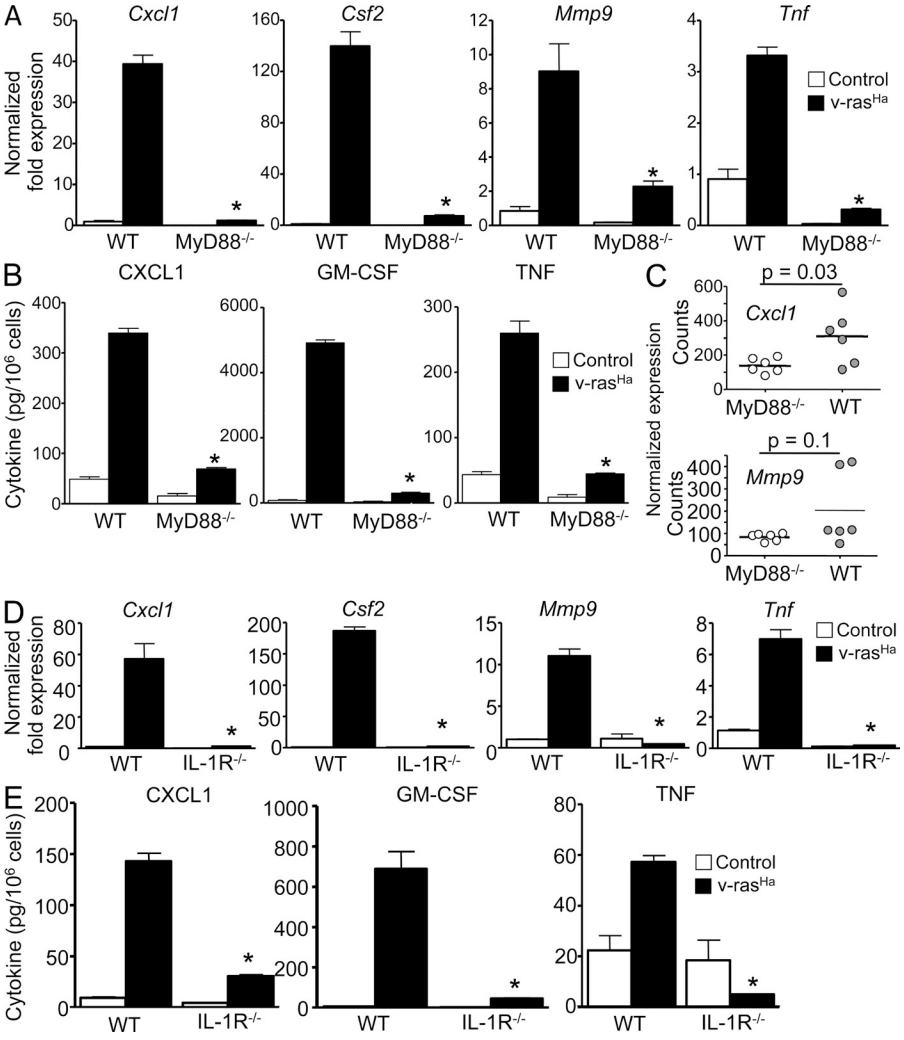

Figure 2. Expression of NF-κB–regulated proinflammatory factors in RAS-transformed keratinocytes requires a functional IL-1–MyD88 axis. (A and D) Real-time PCR analyses 3 d after RAS transduction of *Cxcl1*, *Csf2*, *Mmp9*, and *Tnf* mRNA expression in control and v-ras^{Ha}–transduced keratinocytes (WT and MyD88$^{-/-}$ [A] or IL-1R$^{-/-}$ [D]). (B and E) CXCL1, GM-CSF, and TNF concentrations were determined by ELISA in culture supernatants from control and v-ras^{Ha}–transduced keratinocytes (WT and MyD88$^{-/-}$ [B] or IL-1R$^{-/-}$ [E]) 3 d after RAS transduction. Data shown are representative of three independent experiments, and bars represent the mean ± SEM of five replicates. *, $P < 0.05$ between v-ras^{Ha} WT and v-ras^{Ha} gene–deficient strain. (C) NanoString analysis of *Cxcl1* and *Mmp9* mRNA expression in laser capture–microdissected WT and MyD88$^{-/-}$ papillomas from chemically induced skin carcinogenesis. The y axis shows normalized NanoString counts. Each circle represents an independent squamous papilloma. Horizontal bars indicate the mean.

WT or MyD88$^{-/-}$ mice, and chimeras and transplanted controls were subjected to DMBA/TPA. In this study, no tumors developed in the MyD88$^{-/-}$-MyD88$^{-/-}$ transplanted controls (Fig. 1 C). However, cross chimeras indicate that MyD88 is required in both donor BM–derived and radiation-resistant host cells for optimal skin carcinogenesis. Neither cross transfer chimera fully restored or corrected the high tumor yield of the WT-WT autologous transplanted control. To further confirm the role of epidermal MyD88 during skin carcinogenesis, targeted disruption of MyD88 in basal keratinocytes (MyD88$^{\Delta KC}$) was achieved by crossing MyD88$^{fl/fl}$ mice with keratin 5 (K5) Cre recombinase transgenic mice (K5-Cre^{+}; Ramirez et al., 2004). Tumor burden is reduced by 50% in MyD88$^{\Delta KC}$ mice compared with the control mice (Fig. 1 D). This result confirms that keratinocyte-specific ablation of MyD88 is sufficient to confer significant resistance to DMBA-induced skin tumorigenesis. Finally, crossing MyD88$^{fl/fl}$ mice with Vav1-Cre^{+} mice, ensuring MyD88 deletion in all hematopoietic lineages (MyD88$^{\Delta BM}$; de Boer et al., 2003), demonstrates the equally important contribution of MyD88 from BM-derived cells (Fig. 1 E). Collectively, those results demonstrate that both keratinocyte and BM MyD88–expressing cells contribute to skin carcinogenesis. Sensitivity to skin carcinogenesis ultimately reflects the intrinsic properties of the incipient cells (keratinocytes carrying a mutated H-ras or RAS-keratinocytes) but also the sensitivity to tumor promotion resulting from the cross talk between epidermal cells, the tumor stroma, and the immune system. Little is known regarding the intrinsic role of MyD88 in cancer cells; for that reason we chose to investigate the contribution of MyD88 to the RAS-keratinocyte phenotype.

Expression of protumorigenic factors in RAS-transformed keratinocytes requires a functional IL-1R–MyD88 signal

We have previously reported that oncogenic RAS activates an autocrine loop through the NF-κB–mediated up-regulation of CXCR2 ligands (CXCL1/2/6) binding to CXCR2 on keratinocytes, therefore contributing to tumor cell migration and the chemokine milieu in the microenvironment. Activation of keratinocyte CXCR2 is essential for tumor formation (Cataisson et al., 2009). We tested whether MyD88 was required for RAS-transduced keratinocytes to produce factors important in the tumor microenvironment (Moore et al., 1999; Coussens et al., 2000; Obermueller et al., 2004). Up-regulation of *Cxcl1*, *Csf2*, *Tnf*, and *Mmp9* messenger RNA (mRNA) by oncogenic RAS in transformed

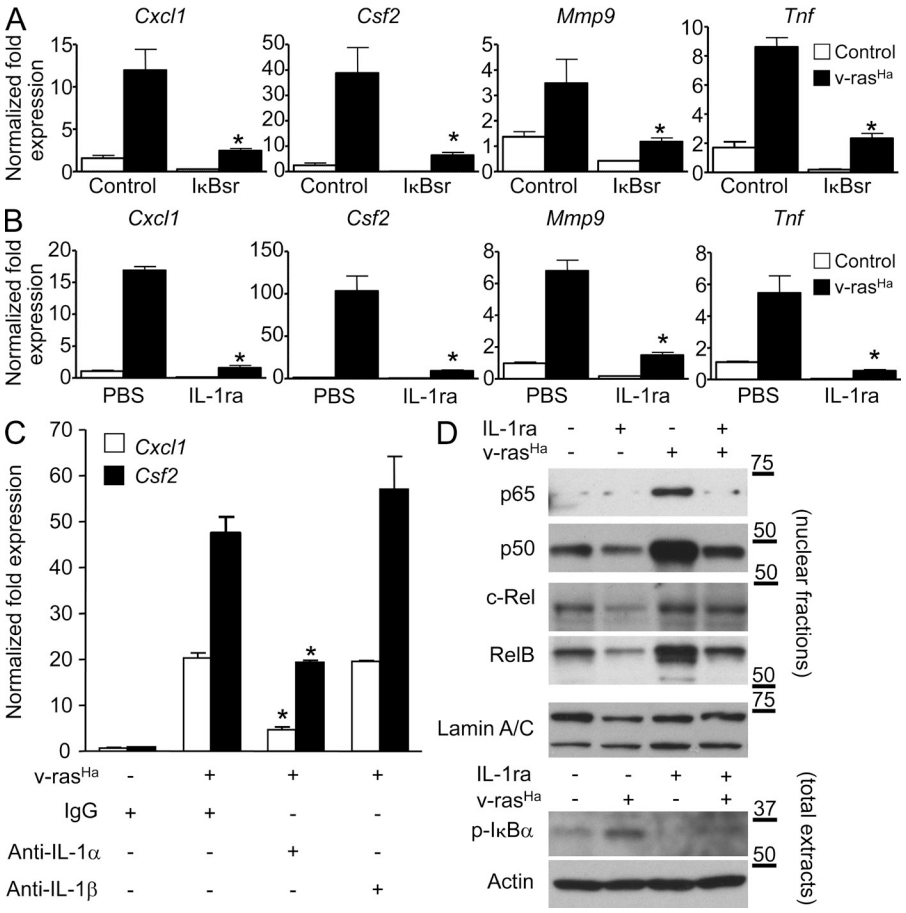

Figure 3. IL-1α autocrine signaling contributes to oncogenic RAS-mediated activation of NF-κB–regulated genes. (A) Real-time PCR analysis of *Cxcl1*, *Csf2*, *Mmp9*, and *Tnf* mRNA expression in control keratinocytes or keratinocytes transduced for 3 d with v-ras^{Ha} and infected with A-CMV (control) or degradation-resistant IκBα (IκBsr) adenovirus to block NF-κB activity for an additional 2 d. *, $P < 0.05$ between v-ras^{Ha} control adenovirus and v-ras^{Ha} IκBsr adenovirus. (B) Real-time PCR analysis of *Cxcl1*, *Csf2*, *Mmp9*, and *Tnf* mRNA expression in control or v-ras^{Ha}–transduced WT keratinocytes treated with PBS or IL-1R antagonist (IL-1ra, Anakinra). *, $P < 0.05$ between v-ras^{Ha} PBS and v-ras^{Ha} IL-1ra. (A and B) Data shown are representative of three independent experiments, and bars represent the mean ± SEM of three replicates. (C) Real-time PCR analysis of *Cxcl1* and *Csf2* mRNA expression in control and v-ras^{Ha}–transduced keratinocytes treated with control IgG, IL-1α neutralizing antibodies, or IL-1β neutralizing antibodies. Data shown are representative of two independent experiments, and bars represent the mean ± SEM of three replicates. *, $P < 0.05$ between v-ras^{Ha} + IgG and v-ras^{Ha} + anti–IL-1α. (D) Nuclear extracts (top) or total cell extract (bottom) from primary keratinocytes transduced for 3 d with v-ras^{Ha} in the presence or absence of IL-1ra (Anakinra) were analyzed by Western blotting. The picture is representative of three independent experiments. Molecular mass is indicated in kilodaltons.

keratinocytes was nearly absent with MyD88 deficiency (Fig. 2 A), as was the release of CXCL1, GM-CSF, and TNF in culture supernatants (Fig. 2 B). A similar phenotype was observed in IL-1R–deficient RAS-keratinocytes (Fig. 2, D and E). The expression of *Cxcl1* mRNAs was also reduced in the laser microdissected epithelial compartment of Myd88$^{-/-}$ papillomas compared with their WT counterpart (Fig. 2 C), whereas the reduction in *Mmp9* did not reach statistical significance. In those same papillomas, the infiltration of CD45- and F4/80-positive cells was similar, as detected by immunostaining (not depicted).

IL-1α autocrine signaling contributes to oncogenic RAS–mediated activation of NF-κB

Blocking NF-κB transcriptional activity by introducing a dominant-negative mutant IκBα adenovirus (IκBsr) also reduced oncogenic RAS–mediated induction of *Cxcl1*, *Csf2*, *Tnf*, and *Mmp9* (Fig. 3 A; Cataisson et al., 2009). Similarly, blocking extracellular IL-1 activity by treating WT control and RAS-keratinocytes with IL-1R antagonist (IL-1ra; Anakinra) also prevented the induction of those genes by oncogenic RAS (Fig. 3 B), suggesting an autocrine loop through the IL-1R. However, only antibodies against IL-1α but not IL-1β could prevent RAS-mediated induction of *Cxcl1* and *Csf2* (Fig. 3 C). Anakinra (IL-1ra) treatment blocked RAS-mediated phosphorylation of IκBα (Fig. 3 D, bottom) and nuclear translocation of p65, p50, and RelB, whereas nuclear c-Rel accumulation in RAS-transduced keratinocytes was unchanged (Fig. 3 D, top). Collectively, these results suggest that in RAS-transformed keratinocytes, IL-1α signaling through IL-1R and MyD88 is required for the activation of NF-κB–regulated genes.

MyD88 deficiency and lack of IL-1R signaling do not impair EGFR autocrine signaling

Previous studies have shown that oncogenic RAS also establishes an essential autocrine loop through the EGFR in murine keratinocytes by up-regulating EGFR ligands (Dlugosz et al., 1995) and that disruption of autocrine EGFR signaling abolishes the NF-κB–mediated induction of CXCL1 and CXCL2 (Cataisson et al., 2009) and reduces tumor formation (Dlugosz et al., 1997). It was also reported that MyD88 was necessary for MAPK activation in fibroblasts in vitro (Coste et al., 2010). Blocking IL-1 activity with IL-1ra in RAS-transduced keratinocytes had no effect on cell proliferation as measured by thymidine incorporation under proliferating culture conditions (Fig. 4 A) and RAS-mediated activation of EGFR (Fig. 4 B). Also, induction of the EGFR ligands *Btc*, *Areg*, and *Hbegf* was maintained in both MyD88-null

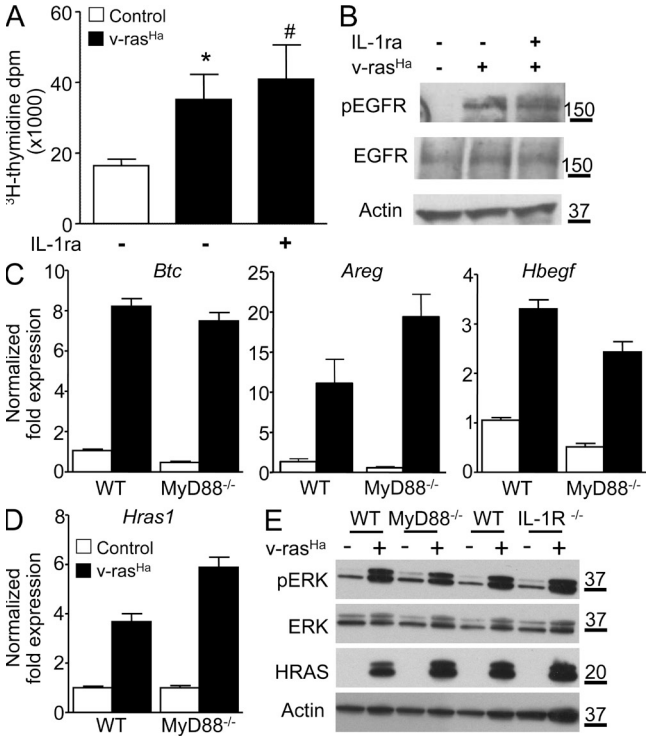

Figure 4. The EGFR autocrine loop is intact in RAS-transformed MyD88-deficient keratinocytes. (A) Tritiated thymidine incorporation was measured in control and v-ras^{Ha}–transduced WT keratinocyte cultures treated with IL-1ra for 3 d. Data shown are representative of three independent experiments, and bars represent the mean ± SEM value of four replicates. *, $P < 0.05$ between v-ras^{Ha} and control; #, no significant difference between v-ras^{Ha} − IL-1ra and v-ras^{Ha} + IL-1ra. (B) Total cell extract from primary keratinocytes transduced for 3 d with v-ras^{Ha} in the presence or absence of IL-1ra (Anakinra) was analyzed by Western blotting for phospho-EGFR (Tyr1068), total EGFR, and actin as loading control. The picture is representative of three independent experiments. (C) Real-time PCR analysis of *Btc* (*betacellulin*), *Areg* (*amphiregulin*), and *Hbegf* (*heparin-binding EGF-like growth factor*) in control and v-ras^{Ha}–transduced keratinocytes (WT and MyD88$^{-/-}$) 3 d after RAS transduction. (D) Real-time PCR analysis of *Hras1* (*H-ras*) in control and v-ras^{Ha}–transduced WT and MyD88$^{-/-}$ keratinocytes. (C and D) Data shown are representative of three independent experiments, and bars represent the mean ± SEM of three replicates. (E) Total cell extract from MyD88$^{-/-}$ and IL-1R$^{-/-}$ primary keratinocytes and their respective controls transduced for 3 d with v-ras^{Ha} were analyzed by Western blotting for phospho-ERK, total ERK, H-ras, and actin as loading control. The picture is representative of two independent experiments. (B and E) Molecular mass is indicated in kilodaltons.

and WT keratinocytes expressing similar levels of oncogenic RAS (Fig. 4, C and D). Activation of ERK was similar in ras-keratinocytes deficient for MyD88 or IL-1R when compared with their WT counterpart (Fig. 4 E). Thus, MyD88 deficiency does not impair EGFR autocrine signaling but rather prevents IL-1R downstream signaling in the oncogenic cascade. Collectively, these results suggest that IL-1R–MyD88 signaling is required for the proper induction of protumorigenic factors in RAS-transformed keratinocytes.

IL-1α–mediated activation of NF-κB contributes to the RAS-initiated differentiation phenotype of keratinocytes

To gain further understanding of IL-1α function in RAS-transformed keratinocytes, we performed a microarray-based gene expression analysis comparing RAS-transduced cultured keratinocytes in the presence or absence of Anakinra. Results presented in Table 1 show the top 30 most up- and down-regulated genes upon blockade of IL-1R signal. Cytokines (*Tnf*, *Csf2*, *Csf3*, and *Il1a*) and chemokines (*Cxcl1*, *Cxcl2*, *Cxcl5*, *Cxcl10*, *Ccl2*, *Ccl5*, *Ccl7*, and *Ccl20*) were among the most down-regulated genes upon IL-1 signal blockade. *Slpi* (*secretory leukocyte peptidase inhibitor*) and *Lcn2* (*lipocalin 2*) were also down-regulated (Fig. 5 A). These genes were reported to be up-regulated in various cancers (Bouchard et al., 2006), *Lcn2* being up-regulated in breast cancer cells through an HER2–NF-κB pathway (Leng et al., 2009). Among the changes associated with the expression of oncogenic RAS in keratinocytes is a characteristic defect in differentiation signaling exemplified by the constitutive down-regulation of suprabasal keratins K1 and K10 (Dlugosz et al., 1994) and their lack of response to calcium-mediated differentiation. Unexpectedly, several genes associated with keratinocyte differentiation as well as cell to cell adhesion and calcium signaling were up-regulated upon IL-1R blockade in RAS-transformed keratinocytes (Table 1 and Fig. S1), including *Calm5* (*calmodulin 5*), *Krt1* and *Krt10* (*keratin 1* and *10*), *Hmr* (*hornerin*), *Dsg1a* (*desmoglein 1 α*), *Cntn2* (*contactin 2*), and *Slurp-1* (*secreted Ly-6/uPAR-related protein 1*). Increased transcript expression for K1 and K10 was confirmed by real-time PCR analysis in both Anakinra-treated and IL-1R–deficient keratinocytes (Fig. 5 B). Furthermore, the induction of K1 and K10 proteins in response to increased extracellular calcium concentration is partially restored in RAS-keratinocytes deficient for IL-1R (Fig. 5 C) or RAS-keratinocytes blocked for NF-κB signaling by transduction with IκBsr (Fig. 5 D). The expression of basal keratin 5 remained unchanged under those same conditions (Fig. 5 C). This observation suggests that autocrine IL-1α signaling contributes to the altered differentiation characteristic of keratinocytes transformed by RAS but does not impact the hyperproliferation associated with tumor formation.

An EGFR–IL-1R–NF-κB axis is created in transformed keratinocytes

We have previously reported that the disruption of autocrine EGFR signaling abolished the NF-κB–mediated induction of CXCL1 and other CXCR2 ligands in RAS-transformed keratinocytes (Cataisson et al., 2009), whereas this current work demonstrates that an IL-1 signal mediates the induction of CXCL1. This suggests that IL-1α is a downstream target of oncogenic RAS and EGFR signaling. Fig. 6 (A and B) indicates that transformation by oncogenic RAS induces both *Il1a* and *Il1b* mRNA and release of IL-1α protein and this is prevented by genetic ablation of EGFR. IL-1β was undetectable in supernatants in all conditions tested (not depicted). Unlike IL-1R (Fig. 2 E), TNFR deficiency does

Table 1. Most up- and down-regulated genes upon blockade of IL-1R signal in RAS-keratinocytes

GenBank accession no.	Symbol	Ratio IL-1Ra/ control	P-value
NM_021480	*Tdh*	5.79	P < 0.01
NM_001008706	*Calm5*	5.74	P < 0.01
NM_010660	*Krt10*	5.25	P < 0.01
NM_008473	*Krt1*	5.08	P < 0.01
NM_183136	*Spink8*	4.91	P < 0.01
NM_031378	*Gsdmc*	4.09	P < 0.01
NM_025416	*Them5*	4.08	P < 0.01
NM_030703	*Cpn1*	3.93	P < 0.01
NM_027548	*Serpinb7*	3.78	P < 0.01
AY027660	*Hrnr*	3.53	P < 0.01
NM_010079	*Dsg1a*	3.42	P < 0.01
NM_177129	*Cntn2*	3.32	P < 0.01
NM_023383	*Aadac*	3.08	P < 0.01
NM_010203	*Fgf5*	3.06	P < 0.01
NM_144936	*Tmem45b*	3.04	P < 0.05
NM_020519	*Slurp1*	3.04	P < 0.01
AY027660	*Hrnr*	2.91	P < 0.01
NM_027416	*Calml3*	2.91	P < 0.01
NM_007574	*C1qc*	2.89	P < 0.05
NM_172806.2	*Btbd7*	2.81	P < 0.05
NM_178924	*Upk1b*	2.72	P < 0.05
NM_008524	*Lum*	2.68	P < 0.01
NM_027286	*Ace2*	2.65	P < 0.01
NM_028882	*Sema3d*	2.61	P < 0.01
NM_033648	*Fxyd4*	2.61	P < 0.01
NM_008190	*Guca2a*	2.52	P < 0.01
NM_007717	*Cmah*	2.52	P < 0.01
BC030317	*Lrrc17*	2.51	P < 0.01
NM_008360	*Il18*	2.51	P < 0.01
NM_018830	*Asah2*	2.50	P < 0.05
NM_178381	*Ano9*	2.49	P < 0.01
NM_010554	*Il1a*	0.35	P < 0.01
NM_010809	*Mmp3*	0.34	P < 0.01
NM_021274	*Cxcl10*	0.34	P < 0.01
NM_007621	*Cbr2*	0.33	P < 0.01
NM_013519	*Foxc2*	0.33	P < 0.01
NM_007778	*Csf1*	0.32	P < 0.01
NM_013599	*Mmp9*	0.31	P < 0.01
NM_013653	*Ccl5*	0.30	P < 0.01
NM_153159	*Zc3h12a*	0.30	P < 0.05
NM_001029929	*Zmynd15*	0.30	P < 0.01
BC033508	*Ccl5*	0.30	P < 0.01
NM_030601	*Clca2*	0.28	P < 0.01
NM_011414	*Slpi*	0.27	P < 0.01
NM_009899	*Clca1*	0.26	P < 0.01
NM_145857	*Nod2*	0.26	P < 0.01
NM_172922	*Ankk1*	0.24	P < 0.01
NM_021301	*Slc15a2*	0.24	P < 0.01
NM_009890	*Ch25h*	0.22	P < 0.01
NM_007825	*Cyp7b1*	0.22	P < 0.01
NM_009969	*Csf2*	0.20	P < 0.01
NM_013654	*Ccl7*	0.18	P < 0.05
NM_013693	*Tnf*	0.16	P < 0.01
NM_007752	*Cp*	0.13	P < 0.01
NM_008176	*Cxcl1*	0.12	P < 0.01
NM_009778	*C3*	0.11	P < 0.01
NM_011333	*Ccl2*	0.11	P < 0.01
NM_009971	*Csf3*	0.10	P < 0.01
NM_016960	*Ccl20*	0.09	P < 0.01
NM_009140	*Cxcl2*	0.09	P < 0.05
NM_008491	*Lcn2*	0.04	P < 0.01
NM_009141	*Cxcl5*	0.03	P < 0.01

The differential gene list between the RAS-keratinocytes treated with IL-1ra versus RAS-keratinocyte control group was generated using limma R package with two different cutoffs for p-values.

not prevent the induction of CXCL1 by oncogenic RAS in keratinocytes (Fig. 6 C). Our results suggest that IL-1α can function as a downstream effector of EGFR signaling in keratinocytes. Indeed, IL-1R blockade using Anakinra strongly reduces TGF-α–mediated induction of *Cxcl1* mRNA (Fig. 6 D), indicating a role of IL-1 downstream of EGFR activation (Streicher et al., 2007). MyD88 deficiency (Fig. 6 E), IL-1R deficiency (Fig. 6 F), or NF-κB blockade (Fig. 6 G) strongly reduced IL-1α induction by oncogenic RAS, suggesting that IL-1α is contributing to a self-amplifying loop in RAS-transformed keratinocytes. Finally, induction of IL-1α by oncogenic RAS is potentiated in transgenic keratinocytes overexpressing PKC-α (Fig. 6 H). This observation is in accordance with PKC-α being the specific isozyme involved in down-modulating expression of keratins K1 and K10 in RAS-transformed keratinocytes (Dlugosz et al., 1994).

MyD88 deficiency but not IL-1 blockade prevents RAS-keratinocytes from forming tumors in vivo

To directly test the role of keratinocyte MyD88 on the RAS-keratinocyte phenotype in vivo, primary keratinocytes from MyD88$^{-/-}$ and WT mice were transduced with the v-*ras*^{Ha} retrovirus and transplanted to a prepared orthotopic graft site on the midback region of nude mice (Lichti et al., 2008). By this approach, tumor formation is dependent solely on the grafted keratinocyte MyD88 as the host is competent for MyD88 expression. Both groups developed squamous papillomas (Fig. 7 A), but tumor growth was minimal in the absence of keratinocyte MyD88 (Fig. 7, B and G). The number of apoptotic cells detected by TUNEL staining (Fig. 7 C) as well as the number of proliferating cells (BrDU positive) were similar in papillomas originating from either genotype (Fig. 7 D). However, in papillomas arising from MyD88-deficient RAS-keratinocytes, the vascular density was reduced by 30% as

assayed by CD31 staining (Fig. 7, E and F). Of note, when orthografts were implanted in the adipose-rich very vascular interscapular region, developing papillomas were larger and vascular density and tumor growth were similar for WT and MyD88$^{-/-}$ tumors (Fig. 7 G and not depicted). It is therefore likely that the papilloma growth difference was related in part to a defective paracrine signaling from tumor cells to elicit an angiogenic response by the host at the midback location. When RAS-keratinocytes from IL-1R$^{-/-}$ and WT mice were implanted midback, developing papillomas were very small in both groups, and no difference among the groups was detected for tumor growth (Fig. 7, G and H), the number of proliferating cells, or vascular density (Fig. 7 I). Similarly, a systemic blockade of IL-1R signaling (using Anakinra in vivo) had no impact on papilloma growth of WT orthotopic grafts (Fig. 7 J). Collectively, those results suggest that reduced growth of orthotopic grafts of MyD88$^{-/-}$ RAS-keratinocytes cannot be attributed solely to intrinsic IL-1R signaling in vivo. Although the identity of the factors that distinguish IL-1α and MyD88 signaling for tumor formation in vivo remain to be determined, these results demonstrate a cancer cell–intrinsic function for MyD88 and IL-1R signaling during squamous carcinogenesis.

DISCUSSION

The multistage evolution of squamous cancer into distinct stages of initiation, promotion, premalignant progression, and malignant conversion characterizes mouse skin carcinogenesis. This model is advantageous because tumor development is quantitative, visible, and time dependent and phenotypic markers have been established to assess tumor progression (Abel et al., 2009). Most alluring is the ability to correlate initiation and phenotypic progression with specific genetic and biochemical pathways (Dlugosz et al., 2002). *Ras* gene mutations are integral to and sufficient for skin tumor initiation in mice. Similarly *RAS* gene mutations are early and frequent events in human cancers where they have been detected in 90% of pancreatic cancers, 50% of colon cancers, 25% of lung cancers, and up to 20% of skin tumors (Pierceall et al., 1991; Spencer et al., 1995; Schubbert et al., 2007; Pylayeva-Gupta et al., 2011). Activation of RAS through epigenetic regulation is even more frequent in skin tumors (Dajee et al., 2003; Khavari, 2006). Thus, it is imperative to understand the phenotypic consequences of RAS activation in normal epithelial cells. Mouse skin papillomas develop as a clonal expansion of initiated cells and thus display the cellular changes required for initiation, including enhanced proliferation and migration, inhibited terminal differentiation, and reduced expression of normal keratinocyte differentiation markers and up-regulation of markers of internal epithelia. In vivo, gene ablation studies have revealed that papilloma formation requires several RAS effector signaling pathways including raf, ralGDS, and PI3K (González-García et al., 2005; Gupta et al., 2007; Ehrenreiter et al., 2009). However, the distal effectors that are required to produce the papilloma

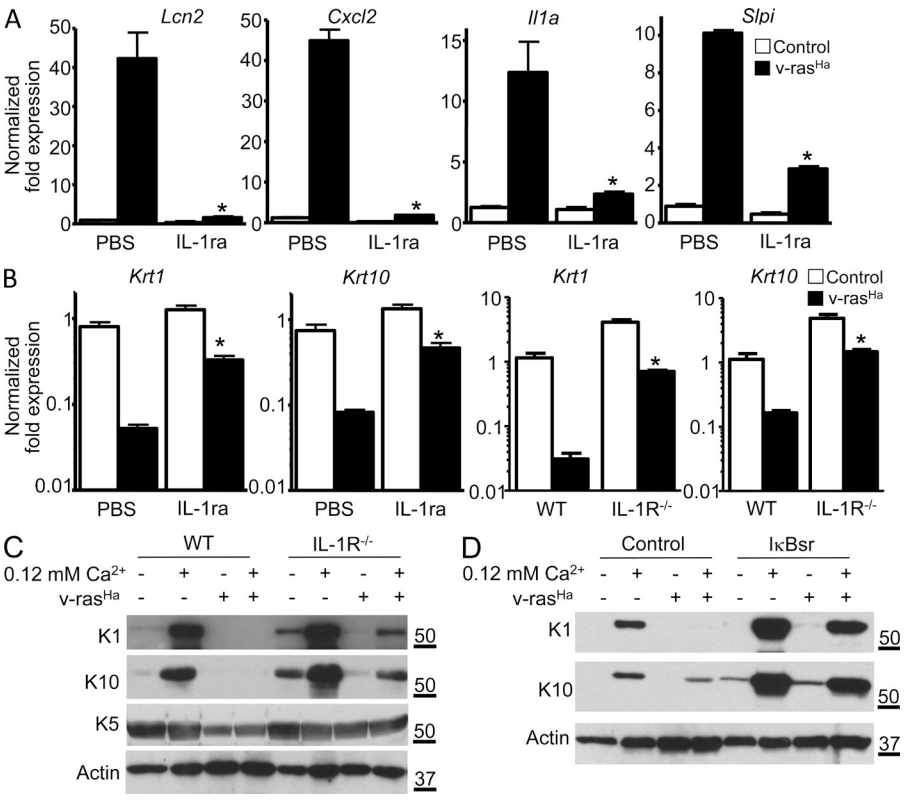

Figure 5. IL-1α–mediated activation of NF-κB is responsible for the altered expression of differentiation markers in RAS-transformed keratinocytes. (A) Real-time PCR analysis of *Lcn2*, *Cxcl2*, *Il1a*, and *Slpi* mRNA expression in control or v-ras^{Ha}–transduced WT keratinocytes treated with PBS or IL-1ra (Anakinra). *, $P < 0.05$ between v-ras^{Ha} PBS and v-ras^{Ha} IL-1ra. (B) Real-time PCR analysis of *Krt1* (*keratin 1*) and *Krt10* (*keratin 10*) mRNA expression in control and v-ras^{Ha}–transduced keratinocytes (PBS or IL-1ra treated or IL-1R WT and IL-1R$^{-/-}$) 3 d after RAS transduction. *, $P < 0.05$ between v-ras^{Ha} PBS and v-ras^{Ha} IL-1ra or v-ras^{Ha} IL-1R WT and v-ras^{Ha} IL-1R$^{-/-}$. (A and B) Data shown are representative of three independent experiments, and bars represent the mean ± SEM of three replicates. (C and D) Total SDS cell extracts from control and v-ras^{Ha}–transduced keratinocytes (IL-1R WT and IL-1R$^{-/-}$; C) or WT keratinocytes infected with A-CMV (control) or degradation-resistant IκBα super repressor (IκBsr) adenovirus to block NF-κB activity (D) were analyzed through immunoblotting with specific antibodies for the expression of basal (K5) and early markers of differentiation (K1 and K10). SDS lysates were analyzed from 3-d posttransduction cultures that were maintained in 0.05 or 0.12 mM Ca^{2+} media for an extra 24 h. Data are representative of three independent experiments. Molecular mass is indicated in kilodaltons.

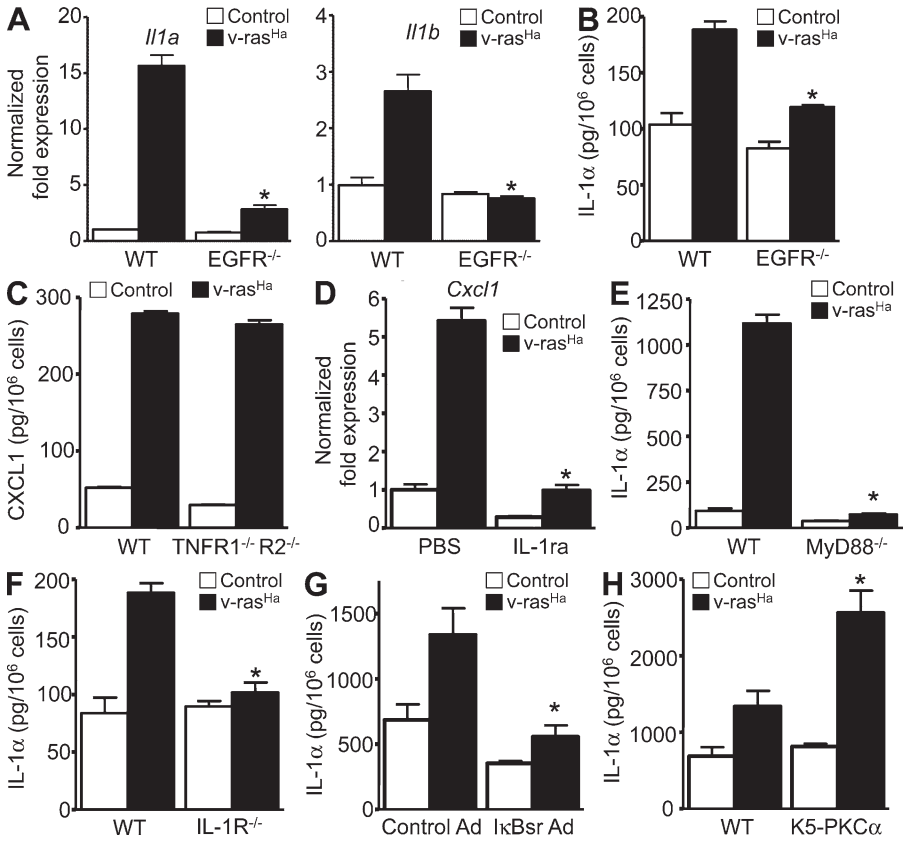

Figure 6. Oncogenic RAS–mediated EGFR–IL-1R signaling loops. (A) Real-time PCR analysis of IL-1α (*Il1a*) and IL-1β (*Il1b*) mRNA expression in control or v-ras^{Ha}–transduced WT and EGFR$^{-/-}$ keratinocytes. (B) Culture supernatants from WT or EGFR$^{-/-}$ primary keratinocytes were collected after control or v-ras^{Ha} transduction. IL-1α concentrations were determined by ELISA. *, $P < 0.05$ between v-ras^{Ha} EGFR WT and v-ras^{Ha} EGFR$^{-/-}$. (C) Culture supernatants from WT and TNFR1$^{-/-}$/TNFR2$^{-/-}$ primary keratinocytes were collected after control or v-ras^{Ha} transduction. CXCL1 concentrations were determined by ELISA. (D) Real-time PCR analysis of CXCL1 (*Cxcl1*) mRNA expression in keratinocytes pretreated with PBS or IL-1ra (Anakinra) for 1 h before TGF-α stimulation for an extra hour. *, $P < 0.05$ between TGF-α treatment − IL-1ra and TGF-α treatment + IL-1ra. (E and F) Culture supernatants from WT or MyD88$^{-/-}$ primary keratinocytes were collected after control or v-ras^{Ha} transduction. IL-1α concentrations were determined by ELISA in culture supernatants from control and v-ras^{Ha}–transduced keratinocytes (WT and MyD88$^{-/-}$ [E] or IL-1R$^{-/-}$ [F]) 3 d after v-ras^{Ha} transduction. *, $P < 0.05$ between v-ras^{Ha} WT and v-ras^{Ha} gene–deficient strain. (G) Culture supernatant collected from control or v-ras^{Ha}–transduced keratinocytes infected with A-CMV (control Ad) or degradation-resistant IκBα (IκBsr Ad) adenovirus to block NF-κB activity. IL-1α concentrations were determined by ELISA. *, $P < 0.05$ between v-ras^{Ha} control Ad and v-ras^{Ha} IκBsr Ad. (H) Culture supernatants from WT or primary keratinocytes from mice overexpressing PKC-α (K5-PKCα) were collected after control or v-ras^{Ha} transduction. IL-1α concentrations were determined by ELISA. *, $P < 0.05$ between v-ras^{Ha} WT and v-ras^{Ha} K5-PKCα. Data shown are representative of two (C and H) to three (A, B, and D–G) independent experiments, and bars represent the mean ± SEM of three (A, B, and D–H) to five (C) replicates.

phenotype have been dissected using cultured mouse keratinocytes transduced with an oncogenic RAS vector (Roop et al., 1986). These studies have revealed several autocrine loops essential for initiation. Up-regulation of EGFR ligands and EGFR activity stimulates proliferation and activates the SRC pathway to tyrosine phosphorylate PKC-δ, reducing its role as an essential component of the keratinocyte death pathway, thus inhibiting the terminal stage of differentiation (Denning et al., 1996; Joseloff et al., 2002). Through the EGFR stimulation of phospholipase C, enhanced PKC-α activity alters keratinocyte gene expression through AP-1 and NF-κB (Dlugosz et al., 1994; Cataisson et al., 2009). This establishes a second autocrine loop through NF-κB–mediated up-regulation of ligands for CXCR2 that act on keratinocytes CXCR2 to stimulate migration (Cataisson et al., 2009). RAS-transformed CXCR2-deficient keratinocytes failed to produce tumors in vivo (Cataisson et al., 2009), suggesting a protumorigenic function for CXCR2 ligands in keratinocytes during skin carcinogenesis (O'Hayer et al., 2009). CXCR2 ligands contain an ELR motif and have strong paracrine proangiogenic properties in human cancer cell xenografts (Sparmann and Bar-Sagi, 2004; Wang et al., 2006), grafted murine SCC cells (Loukinova et al., 2000), melanoma cells (Horton et al., 2007), and animal models of lung cancer (Keane et al., 2004; Wislez et al., 2006). We and others have also demonstrated that autocrine CXCR2 signaling promotes keratinocyte tumorigenic behavior (Miyazaki et al., 2006; Cataisson et al., 2009). Consequently, antagonizing CXCR2 activity in tumors might be of therapeutic value in squamous cancers (Yeudall and Miyazaki, 2007).

The current study has now revealed a third autocrine loop that connects this EGFR–PKC-α–NF-κB axis. Tumor initiation by oncogenic RAS, through EGFR and PKC-α, causes release of IL-1α, activation of the IL-1R and association with MyD88, phosphorylation of IκBα, and nuclear translocation of p65, p50, and RelB, activating NF-κB transcriptional activity. Among the downstream effectors are CXCR2 ligands and the suppression of keratinocyte differentiation markers that characterize the initiated phenotype. These new findings now link RAS activation to NF-κB in an exploitable pathway.

Our data provide a molecular link between oncogenic RAS and the activation of NF-κB in keratinocytes, therefore explaining in part the inflammation/innate immunity

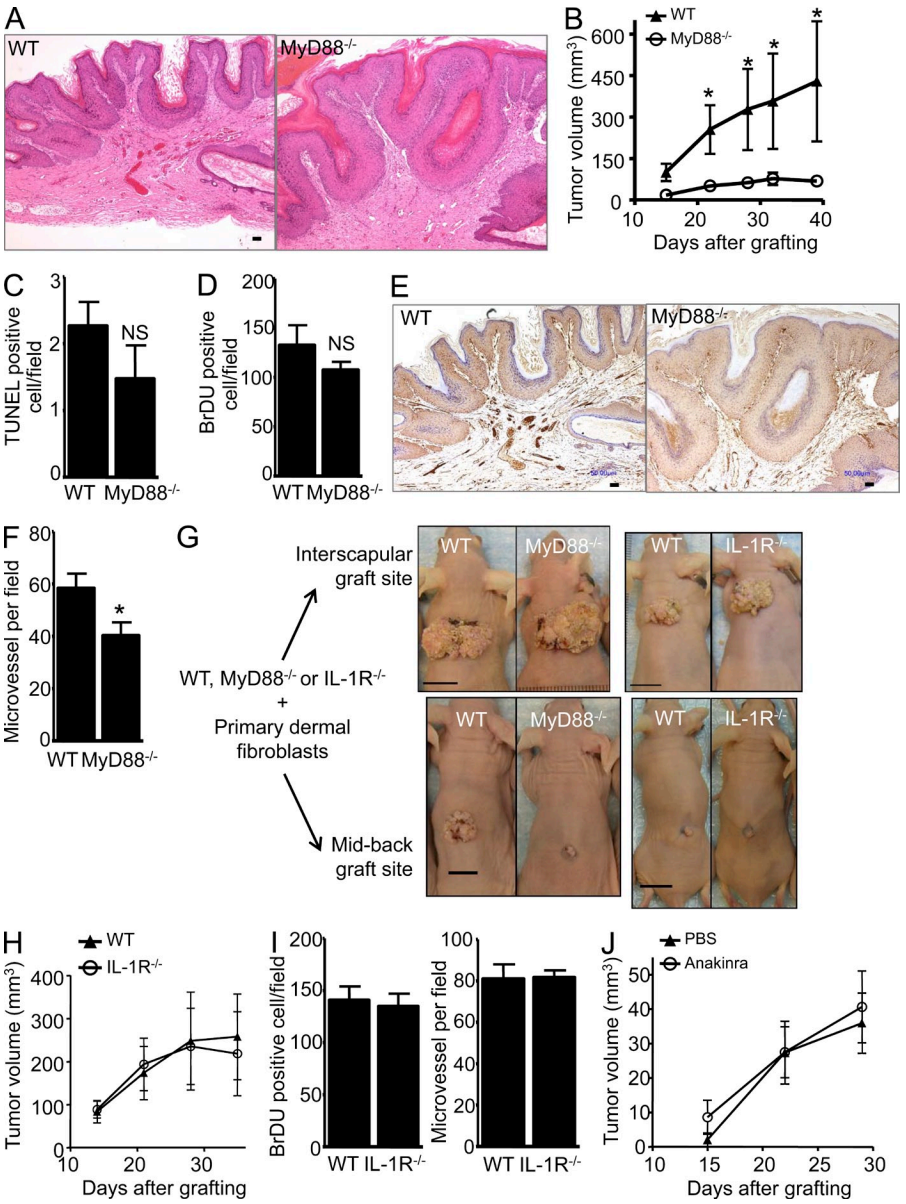

Figure 7. MyD88 deficiency impairs growth of v-ras^{Ha}–induced squamous tumors through an IL-1–independent signal. (A and B) Representative H&E micrograph of WT and MyD88$^{-/-}$ orthotopic grafts. WT or MyD88$^{-/-}$ primary v-ras^{Ha}–transduced keratinocytes combined with MyD88 WT dermal fibroblasts were grafted onto nude mice (A), and mean tumor volume was calculated as described in Materials and methods (B). Data shown are representative of two independent experiments and are reported as mean ± SEM. *, $P < 0.05$ between the WT and MyD88$^{-/-}$ group. Each group contains eight to nine mice. Only mice bearing tumors were included in this figure. (C) Tumors from A were stained for markers associated with tumor growth. Apoptotic cells were identified using the ApopTag kit, which stains nuclei containing nicked DNA. Positive nuclei were counted in five to seven randomly selected regions. (D) BrdU-labeled nuclei were detected in stained sections of tumors from mice injected with BrdU 1 h before sacrifice and similarly counted. (C and D) Data are reported as mean ± SEM. NS, difference not statistically significant between the WT and MyD88$^{-/-}$ groups. (E) Immunostaining for CD31 antigen outlining blood vessels within tumors originating from WT or MyD88$^{-/-}$ v-ras^{Ha}–transduced keratinocytes. (F) Microvessel density was determined based on the number of CD31^{+} cells in at least five fields per tumor originating from MyD88 WT or MyD88$^{-/-}$ v-ras^{Ha}–transduced keratinocytes. Data are reported as mean ± SEM. *, $P < 0.05$ between the WT and MyD88$^{-/-}$ groups. (G) Representative photographs of orthotopic grafts at the interscapular site (top) and mid-back site (bottom). 4 million RAS-keratinocytes were mixed with 5 million SENCAR mouse primary dermal fibroblasts before grafting. WT RAS-keratinocytes from C57BL/6J mice (IL-1R colony) underperform compared with WT RAS-keratinocytes from C57BL/6NCr mice (MyD88 colony) for both graft sites. In addition, the percentage of success of RAS-keratinocyte grafts from C57BL/6J mice at the midback graft site was very poor. WT and MyD88$^{-/-}$ and IL-1R$^{-/-}$ keratinocytes were derived from littermate pups. Grafting data presented in B, H, and J were performed at the midback site. Bars: (A and E) 50 µm; (G) 10 mm. (H) IL-1R WT or IL-1R$^{-/-}$ primary v-ras^{Ha}–transduced keratinocytes combined with SENCAR WT dermal fibroblasts were grafted onto nude mice, and mean tumor volume was calculated as described in Materials and methods. Each group contains three to five mice. Data shown are representative of two independent experiments and are reported as mean ± SEM. (I) BrdU-labeled nuclei and immunostaining for CD31 were analyzed as described for D and F. (J) v-ras^{Ha}–transduced keratinocytes (PBS or IL-1ra [Anakinra] treated) combined with SENCAR MyD88 WT dermal fibroblasts were grafted onto nude mice, and mean tumor volume was calculated as described in Materials and methods. PBS or Anakinra was administered daily by intraperitoneal injection starting the day after the surgical procedure for the duration of the experiment. Each group contains four to five mice. Data shown are representative of two independent experiments and are reported as mean ± SEM.

signature triggered by oncogene transformation in epithelial cells. IL-1α establishes a positive feedback loop to reinforce the expression of protumorigenic factors at least in vitro. The protumorigenic role of IL-1 in cancer has been largely attributed to the IL-1β activity within the tumor microenvironment (Apte et al., 2006), although hepatocyte-produced IL-1α contributes to carcinogen-induced liver tumorigenesis (Sakurai et al., 2008). It is well established that IL-1 activity derived from the tumor cells or infiltrating immune cells has the ability to turn on an angiogenic switch in the tumor microenvironment (Liss et al., 2001; Saijo et al., 2002; Nakao et al., 2005). As such, continuous delivery in vivo of

IL-1ra reduced the growth of fibrosarcomas (Bar et al., 2004), and Anakinra treatment of melanoma, lung, and colon adenocarcinoma xenografts decreased their growth, blood vessel counts, and IL-8 expression (Elaraj et al., 2006). Our data indicate that IL-1 blockade in RAS-keratinocytes was not sufficient to prevent papilloma formation in an orthograft model, although the constitutive absence of IL-1R signaling in mice did reduce tumor multiplicity in the two-stage chemical carcinogenesis model in vivo consistent with a previous study (Coste et al., 2010). This divergence in the two models suggests that host factors contribute to tumor formation in grafts. For example, another member of the Toll-like receptor/IL-1 receptor superfamily provided by the host stroma or intrinsic to the tumor cells in the orthograft model can compensate in vivo for loss of IL-1R signaling in keratinocytes. One can only speculate on the nature of that signal in RAS-keratinocytes based on skin carcinogenesis performed so far. TLR4 activation by HMGB1 appears to have a protumorigenic function during skin carcinogenesis, but TLR2, TLR9 (Mittal et al., 2010), and IL-18 (unpublished data) do not. The contribution of IL-33 and IL-36 members with agonist function during skin carcinogenesis is not known. Of note, IL-36α (formerly referred to IL1-F6) has a proinflammatory function in the skin (Blumberg et al., 2007), and its receptor IL-36R is highly expressed on keratinocytes (Vigne et al., 2011). In the two-stage model in vivo, tumor yield is associated with the inflammation that characterizes the tumor promotion phase of papilloma formation (Rundhaug and Fischer, 2010). Tumor promoters like TPA increase IL-1α expression in the skin in vivo (Lee et al., 1993). Neutralizing antibody targeting IL-1α inhibits TPA-induced vascular permeability, immune cell infiltration, and epidermal hyperplasia, further establishing the protumorigenic role of IL-1 (Lee et al., 1994). Blockade of IL-1 also reduces papilloma incidence caused by inflammation secondary to wounding (Arwert et al., 2010).

One consequence of Ras-mediated IL-1 signaling and MyD88 activation is the up-regulation of angiogenic factors, particularly CXCR2 ligands. The orthograft experiments (Fig. 7) revealed that these factors are important for papilloma formation as vascular density was reduced in MyD88-deficient Ras-keratinocytes where papilloma growth was minimal when keratinocytes were placed on the poorly vascularized midback, but papilloma growth was enhanced by grafting in the vessel-rich interscapular fat pad. In contrast, tumor growth was very poor in both WT and IL-1R–deficient Ras-keratinocytes in the midback, suggesting the genetic background of the donor keratinocytes (C57BL/6J) influences tumor growth. Nevertheless, the inability of Anakinra to reduce growth of WT Ras-keratinocytes in orthografts suggests that a deficiency in IL-1R signaling in ras-transformed papilloma cells can be compensated in vivo.

Our data demonstrate the reliance on autocrine IL-1 signaling for oncogenic RAS-induced NF-κB activity and implicate NF-κB in the differentiation defect characteristic of RAS-keratinocytes. Primary mouse keratinocytes expressing oncogenic RAS respond abnormally to signals for terminal differentiation: the level of the differentiation-associated keratins (K1 and K10) is frequently reduced in benign papillomas (Huitfeldt et al., 1991; Sundberg et al., 1994), and Ca^{2+} fails to induce K1 and K10 in vitro after activation of RAS in keratinocytes (Roop et al., 1987; Cheng et al., 1990; Dlugosz et al., 1994). We now show the participation of NF-κB signaling as an intrinsic modifier of this differentiation program. This potentially could also form the basis for the loss of K1 and K10 expression as benign papillomas progress to malignancy under conditions where NF-κB activity is known to be elevated further (Loercher et al., 2004). Interestingly, oncogenic RAS alters keratinocyte differentiation by altering the function of the PKC signaling pathway, and PKC-α is the specific isozyme involved in down-modulating expression of keratins K1 and K10 (Dlugosz et al., 1994). Several instances of NF-κB directly mediating gene transcription silencing have been reported, although an analysis of the genes down-regulated by IL-1α did not consistently reveal the presence of NF-κB consensus elements (unpublished data), and thus, both direct and indirect effects might be involved. Although *Il1a* gene expression is regulated through a self-amplifying mechanism in RAS-transfected cells, it is not dependent only on NF-κB activation. We observed that keratinocytes overexpressing PKC-α produce more IL-1α compared with their WT control, suggesting that PKC-α signaling could be implicated in the induction or release of IL-1α, further connecting IL-1α and altered keratinocyte differentiation.

Overall our data reinforce the hypothesis of an oncogene-driven connection between inflammation and cancer (Borrello et al., 2008). Several oncogenes including *RAS*, *RET*, and *MYC* have now been demonstrated to be responsible not only for cell neoplastic transformation but also to establish intrinsic inflammatory pathways, establishing a protumorigenic microenvironment largely responsible for tumor angiogenesis (Borrello et al., 2008). Although oncogenic mutations have been reported for MyD88 in human lymphoma (Ngo et al., 2011), our study demonstrates a cancer cell–intrinsic function for MyD88 during skin carcinogenesis. We now clearly establish that NF-κB activation through MyD88 represents an essential positive feedback mechanism for the induction and maintenance of the RAS-mediated inflammatory program as reported also in other types of tumors. Unexpectedly, IL-1α signaling is also required for the inhibition of the keratinocyte differentiation program mediated by oncogenic RAS. Thus, inflammatory mediators are not only required for the establishment of a protumoral microenvironment but are also acting in a cell-intrinsic way to allow the full expression of the RAS-induced oncogenic transformation program.

MATERIALS AND METHODS

Materials. Anakinra (Kineret, rh-met–IL-1ra; Amgen) is a recombinant, nonglycosylated form of human IL-1Ra. IL-1ra is provided in prefilled syringes of 100 mg (150 mg/ml). IL-1ra was further diluted in culture medium to a final concentration of 5 μg/ml. IL-1ra, neutralizing antibody against IL-1α (final concentration 2.5 μg/ml; Abcam), or IL-1β (final concentration 5.0 μg/ml; Abcam) was added to cultures 5 h after v-ras^{Ha} transduction and replaced every 48 h. Thymocyte proliferation assay was used

to confirm the specificity of anti–IL-1α and anti–IL-1β neutralizing antibodies. Thymi from 8-wk-old naive BALB/c mice were resected, and single-cell thymocyte suspensions were plated at 1.5×10^6 cells/200 µl per well in RPM1 1640 medium supplemented with 5% vol/vol fetal calf serum, 4, 2-mercaptoethanol (2ME), 0.5 µg/ml concanavalin A, 100 U/ml penicillin, 100 U/ml streptomycin, 50 µg/ml gentamicin, and 200 µg/ml L-glutamine, in the presence or absence of 1 ng/ml recombinant mouse IL-1α or 1 ng/ml recombinant mouse IL-1β. The effect of neutralizing antibodies to murine IL-1α (Abcam) and IL-1β (Abcam) was tested at concentrations ranging from 0.25 to 5 µg/ml. Rabbit IgG was used as control. Cultures were incubated for 72 h and pulsed with 0.5 µCi [^{3}H]thymidine per well for the final 16 h of incubation. Thereafter, samples were harvested, and the radioactivity was determined in a liquid scintillation counter.

Mice and treatments. Mouse experiments were performed under a protocol approved by the National Cancer Institute (NCI) and National Institutes of Health Animal Care and Use Committee. Approximately 1 h before sacrifice, animals were injected with 250–300 µl of a 3-mg/ml solution of BrdU in sterile PBS. Samples were fixed in formalin or IHC zinc fixative (BD) and embedded in paraffin for hematoxylin and eosin (H&E) staining and immunohistochemistry. For BrdU staining, sections were treated as recommended by the manufacturer (Roche) using anti-BrdU-POD antibody (clone BMG 6H8). Apoptosis, CD45, F4/80, and CD31 staining was performed by the Pathology/Histotechnology Laboratory (NCI core facility) using, respectively, ApopTag kit (Millipore) or anti–PECAM-1/CD31 antibody (Santa Cruz Biotechnology, Inc.). The microvascular density was determined by counting the number of CD31-stained cells in at least five fields (400×; Eclipse E400; Nikon) per tumor originated from MyD88 WT or MyD88$^{-/-}$ v-ras^{Ha}–transduced keratinocytes.

Tumor induction experiments. MyD88$^{-/-}$ and IL-1R$^{-/-}$ colonies were, respectively, maintained on C57BL/6NCr and C57BL/6J backgrounds. For the IL-1R set of experiments, WT and −/− were littermates. For the MyD88$^{-/-}$ colony, the genetic match to the C57BL/6NCr was confirmed by microsatellite analysis. The dorsal skin of 7-wk-old mice was shaved with surgical clippers and subsequently checked for the lack of hair growth. Initiation was accomplished by a single topical application of 400 nmol DMBA in 0.2 ml acetone. Promoter treatments with 10 nmol TPA in 0.2 ml acetone, three times weekly, were begun 1 wk after initiation and continued for 20 wk. Skin tumors induced by the initiation-promotion protocol were removed and both frozen and formalin fixed at times from 20 to 40 wk after initiation. The eruption of new skin papillomas was monitored by skin palpation twice weekly. It is of note that in this model, C57BL/6J mice are more susceptible to develop papillomas than C57BL/6NCr mice (Fig. 1). The MyD88$^{flox/flox}$ mice (Kleinridders et al., 2009) were crossed with K5-Cre$^+$ (Ramirez et al., 2004) and Vav1-Cre$^+$ (The Jackson Laboratory) to obtain specific deletion of MyD88 in keratinocytes (MyD88$^{\Delta KC}$) and hematopoietic cells (MyD88$^{\Delta BM}$), respectively. These mice were subjected to two-stage skin carcinogenesis as described above. To establish chimeras, mice received BM cells after myeloablative total body irradiation (1,100 cGy). 7 d before and after irradiation, mice received drinking water containing amoxicillin (125 mg per 250 ml of acid water). After irradiation, mice received 20×10^6 BM cells intravenously. 2 mo after transplantation, the chimerism was tested and mice were subjected to skin painting protocol as described above. IL-18$^{-/-}$ mice were purchased from the Jackson Laboratory.

Nude mouse grafting. On day 3 in culture, MyD88$^{+/+}$, MyD88$^{-/-}$, IL-1R$^{+/+}$, or IL-1R$^{-/-}$ primary keratinocytes were infected with the v-*ras*^{Ha} retrovirus and trypsinized and used for grafting on day 8 as described previously (Lichti et al., 2008). 4 million keratinocytes (for C57BL/6NCr) or 7 million keratinocytes (for C57BL/6J) were mixed with 5 or 8 million SENCAR mouse primary dermal fibroblasts, respectively, (cultured for 1 wk) and grafted onto the back of nude mice on a prepared skin graft site located in the midback region unless specified otherwise (Lichti et al., 2008). Tumor dimensions were measured weekly using calipers, and approximate tumor volumes were determined by multiplying tumor height × length × width. Anakinra was injected daily intraperitoneally at a dosage of 250 mg/kg starting the day after the surgical procedure.

Cell culture. Primary mouse keratinocytes and hair follicle buds were isolated from newborn transgenic (K5–PKC-α) and WT littermate epidermis as described previously (Cataisson et al., 2003; Lichti et al., 2008). EGFR-, MyD88-, and IL-1R–deficient keratinocytes were isolated from pups obtained from respective heterozygous breeding pairs (Threadgill et al., 1995). The use of pups from homozygous mice deficient for TNFR1 and TNFR2 (TNFR1$^{-/-}$TNFR2$^{-/-}$) was previously reported (Cataisson et al., 2005).

Retroviral and adenoviral constructs. The v-*ras*^{Ha} replication–defective ecotropic retrovirus was prepared using ψ2 producer cells (Roop et al., 1986). Retrovirus titers were routinely 10^7 virus/ml. Keratinocytes were infected with v-*ras*^{Ha} retrovirus (here referred to as RAS or oncogenic RAS) on day 3 at a multiplicity of infection of 1 in medium containing 4 µg/ml Polybrene (Sigma-Aldrich). The IκBsr (IκBα super repressor) adenovirus was introduced into primary keratinocytes 2 d after v-*ras*^{Ha} transduction using an adenoviral construct driven by a CMV promoter, and empty adenovirus was used as control (A-CMV). Keratinocytes were adenovirus infected for 30 min in serum-free medium with a multiplicity of infection of 10 viral particles/cell and 4.0 µg/ml Polybrene to enhance uptake. Serum-containing medium was added to the cells for the next 48 h after the infection.

Proliferation assay (thymidine incorporation). Keratinocytes were plated in 24-well tissue culture plates and RAS transduced on day 3. Cells were grown in the presence or absence of IL-1ra (Anakinra) for 3 d while pulsed for the last 4 h with 1 µCi [^{3}H]thymidine (GE Healthcare). Cells were fixed using methanol and acetic acid (in a 3:1 ratio) and solubilized in 5 N NaOH, and incorporated counts were measured using a scintillation counter.

Immunoblotting. Cytoplasmic and nuclear extracts from cultured keratinocytes were prepared using the NE-PER kit (Thermo Fisher Scientific) according to the manufacturer's protocol and supplemented with PMSF and Halt phosphatase inhibitor (Thermo Fisher Scientific). Proteins were quantified by the Bradford method (Bio-Rad Laboratories) and separated by 10% SDS-PAGE. ECL SuperSignal (Thermo Fisher Scientific) system was used for detection. H-RAS antibody (C-20; Santa Cruz Biotechnology, Inc.) was used at 1:500 overnight at 4°C, and phospho-EGFR (Tyr1068), phospho-IκBα (Ser32/36), pERK, and total ERK were used at 1:1,000 overnight at 4°C and purchased from Cell Signaling Technology. For analysis of differentiation markers, cultures were washed once with PBS (Ca^{2+} and Mg^{2+} free), and total cell lysates were prepared using 10 µl/cm^2 lysis buffer (5% SDS and 20% 5-mercaptoethanol in 0.25 M Tris, pH 6.8). Detection of differentiation markers, keratin 1 and 10, has been described previously (Dlugosz and Yuspa, 1993). Rabbit antisera raised against synthetic peptides were used and have been described previously: anti–mouse p50 (no. 1263), p65 (no. 1207), p52 (no. 1495), cRel (no. 1266), and RelB (no. 1319; Rice and Ernst, 1993; Ernst et al., 1995; Whiteside et al., 1997).

RT-PCR analysis and gene expression analysis. RNA was isolated from cultured cells with TRIZOL according to the manufacturer's protocol (Invitrogen). cDNA synthesis, real-time PCR analysis, and primer sequences were previously described (Cataisson et al., 2006, 2009). Laser-microdissected papillomas were used to prepare total cell lysates for NanoString analysis. The nCounter Gene Expression Assay was performed using two specific probes (capture and reporter) for each gene of interest. In brief, 5 µl LCM lysate from each laser-dissected papilloma was hybridized with the designed Reporter CodeSet and Capture ProbeSet (according to the manufacturer's instructions; NanoString Technologies) for direct labeling of mRNAs of interest with molecular barcodes without the use of reverse transcription or amplification. The hybridized samples were recovered with the NanoString Prep Station, and the mRNA molecules were counted with the NanoString nCounter. The resulting counts were corrected by subtracting the mean

value of the negative control (alien probes from the CodeSet, lacking spiked transcript) from the raw counts obtained for each RNA. Values < 0 were considered equal to 1. The corrected raw data were finally normalized using values for the housekeeping genes.

Microarray performance and statistical analysis. Total RNA was harvested from cultured v-ras^{Ha}–transduced keratinocytes in the presence of PBS or Anakinra. Total RNA was extracted using TRIZOL reagent according to the manufacturer's instructions. The microarray processing was performed by GenUs Biosystems Inc. RNA was further purified using RNeasy Min-elute RNA isolation kit (QIAGEN). Total RNA samples were quantitated by UV spectrophotometry (OD260/280). Quality of the total RNA was assessed by using an Agilent Bioanalyzer (Agilent Technologies). First and second strand cDNA was prepared from the total RNA samples. cDNA target was prepared from the DNA template and verified on the Bioanalyzer. cDNA was fragmented to uniform size and hybridized to Agilent Whole Genome 4 × 44K arrays. Slides were washed and scanned on an Agilent G2565 Microarray Scanner. The gProcessSignal of Agilent feature extraction data was normalized using a global median-based method and filtered by the Agilent feature extraction flag "gIswellAboveBG" to eliminate bad probes with signals consistently lower than background across the samples. All of these procedures were performed with customized R scripts (www.r-project.org). The normalized data were then subjected to several methods as follows to derive differential gene lists between the treatment and control groups: (a) limma R package with two different cutoffs for p-values, (b) one-way analysis of variance using Partek Genomic Suite, and (c) SAM method (Tusher et al., 2001). To show the consistency and robustness of the behavior of these lists at pathway level, all of the derived differential lists including up and down lists were subjected to pathway-level enrichment pattern extraction and analysis using in-house tool WPS (Yi et al., 2006) and embedded PPEP analysis pipeline (Yi et al., 2009) using annotation databases from Gene Ontology, BioCarta, MSigDB, WikiPathways, and KEGG Pathways. The enrichment scores (−log10(p-value); p-value is the Fisher's exact test p-value) were computed and shown in the pathway-level heat maps for visualization. The normalized data of selected genes were transformed into z scores before being subjected to clustering for display of heat maps using TM4 MeV from TIGR or Partek Genomic Suite. The microarray data were deposited in the GEO database under accession no. GSE22777.

ELISA. CXCL1, GM-CSF, TNF, and IL-1α levels were quantified from culture supernatants using OptEIA or Quantikine ELISA kit (R&D Systems) according to the manufacturer's protocol.

Statistical analysis. Data were analyzed by Prism software (GraphPad Software), and significance values were assigned through Student's *t* test or one-way analysis of variance with Tukey posttest. $P < 0.05$ was considered to be significant.

Online supplemental material. Fig. S1 shows the gene term association network view of the selected terms or pathways upon blockage of IL-1 signaling in RAS-keratinocytes. Online supplemental material is available at http://www.jem.org/cgi/content/full/jem.20101355/DC1.

The authors thank Andrew Ryscavage (Laboratory of Cancer Biology and Genetics, National Cancer Institute [NCI]) for technical assistance, Marta Custer and Susanna Walters for care of the mouse colonies, Steve Jay (SAIC, NCI Bethesda) for helping with the grafting procedure/tumor measurements, and the Pathology/Histotechnology Laboratory (SAIC-Frederick) for excellent technical assistance.

This work was supported by the Intramural Research Program, Center for Cancer Research, National Cancer Institute, National Institutes of Health.

The authors have no conflicting financial interests to declare.

Submitted: 6 July 2010
Accepted: 30 July 2012

REFERENCES

Abel, E.L., J.M. Angel, K. Kiguchi, and J. DiGiovanni. 2009. Multi-stage chemical carcinogenesis in mouse skin: fundamentals and applications. *Nat. Protoc.* 4:1350–1362. http://dx.doi.org/10.1038/nprot.2009.120

Apte, R.N., S. Dotan, M. Elkabets, M.R. White, E. Reich, Y. Carmi, X. Song, T. Dvozkin, Y. Krelin, and E. Voronov. 2006. The involvement of IL-1 in tumorigenesis, tumor invasiveness, metastasis and tumor-host interactions. *Cancer Metastasis Rev.* 25:387–408. http://dx.doi.org/10.1007/s10555-006-9004-4

Arwert, E.N., R. Lal, S. Quist, I. Rosewell, N. van Rooijen, and F.M. Watt. 2010. Tumor formation initiated by nondividing epidermal cells via an inflammatory infiltrate. *Proc. Natl. Acad. Sci. USA.* 107:19903–19908. http://dx.doi.org/10.1073/pnas.1007404107

Bar, D., R.N. Apte, E. Voronov, C.A. Dinarello, and S. Cohen. 2004. A continuous delivery system of IL-1 receptor antagonist reduces angiogenesis and inhibits tumor development. *FASEB J.* 18:161–163.

Blumberg, H., H. Dinh, E.S. Trueblood, J. Pretorius, D. Kugler, N. Weng, S.T. Kanaly, J.E. Towne, C.R. Willis, M.K. Kuechle, et al. 2007. Opposing activities of two novel members of the IL-1 ligand family regulate skin inflammation. *J. Exp. Med.* 204:2603–2614. http://dx.doi.org/10.1084/jem.20070157

Borrello, M.G., D. Degl'Innocenti, and M.A. Pierotti. 2008. Inflammation and cancer: the oncogene-driven connection. *Cancer Lett.* 267:262–270. http://dx.doi.org/10.1016/j.canlet.2008.03.060

Bouchard, D., D. Morisset, Y. Bourbonnais, and G.M. Tremblay. 2006. Proteins with whey-acidic-protein motifs and cancer. *Lancet Oncol.* 7:167–174. http://dx.doi.org/10.1016/S1470-2045(06)70579-4

Brantsch, K.D., C. Meisner, B. Schönfisch, B. Trilling, J. Wehner-Caroli, M. Röcken, and H. Breuninger. 2008. Analysis of risk factors determining prognosis of cutaneous squamous-cell carcinoma: a prospective study. *Lancet Oncol.* 9:713–720. http://dx.doi.org/10.1016/S1470-2045(08)70178-5

Cataisson, C., E. Joseloff, R. Murillas, A. Wang, C. Atwell, S. Torgerson, M. Gerdes, J. Subleski, J.L. Gao, P.M. Murphy, et al. 2003. Activation of cutaneous protein kinase C alpha induces keratinocyte apoptosis and intraepidermal inflammation by independent signaling pathways. *J. Immunol.* 171:2703–2713.

Cataisson, C., A.J. Pearson, S. Torgerson, S.A. Nedospasov, and S.H. Yuspa. 2005. Protein kinase C alpha-mediated chemotaxis of neutrophils requires NF-kappa B activity but is independent of TNF alpha signaling in mouse skin in vivo. *J. Immunol.* 174:1686–1692.

Cataisson, C., A.J. Pearson, M.Z. Tsien, F. Mascia, J.L. Gao, S. Pastore, and S.H. Yuspa. 2006. CXCR2 ligands and G-CSF mediate PKCalpha-induced intraepidermal inflammation. *J. Clin. Invest.* 116:2757–2766. http://dx.doi.org/10.1172/JCI27514

Cataisson, C., R. Ohman, G. Patel, A. Pearson, M. Tsien, S. Jay, L. Wright, H. Hennings, and S.H. Yuspa. 2009. Inducible cutaneous inflammation reveals a protumorigenic role for keratinocyte CXCR2 in skin carcinogenesis. *Cancer Res.* 69:319–328. http://dx.doi.org/10.1158/0008-5472.CAN-08-2490

Cheng, C., A.E. Kilkenny, D. Roop, and S.H. Yuspa. 1990. The v-ras oncogene inhibits the expression of differentiation markers and facilitates expression of cytokeratins 8 and 18 in mouse keratinocytes. *Mol. Carcinog.* 3:363–373. http://dx.doi.org/10.1002/mc.2940030608

Coste, I., K. Le Corf, A. Kfoury, I. Hmitou, S. Druillennec, P. Hainaut, A. Eychene, S. Lebecque, and T. Renno. 2010. Dual function of MyD88 in RAS signaling and inflammation, leading to mouse and human cell transformation. *J. Clin. Invest.* 120:3663–3667. http://dx.doi.org/10.1172/JCI42771

Coussens, L.M., C.L. Tinkle, D. Hanahan, and Z. Werb. 2000. MMP-9 supplied by bone marrow-derived cells contributes to skin carcinogenesis. *Cell.* 103:481–490. http://dx.doi.org/10.1016/S0092-8674(00)00139-2

Dajee, M., M. Lazarov, J.Y. Zhang, T. Cai, C.L. Green, A.J. Russell, M.P. Marinkovich, S. Tao, Q. Lin, Y. Kubo, and P.A. Khavari. 2003. NF-kappaB blockade and oncogenic Ras trigger invasive human epidermal neoplasia. *Nature.* 421:639–643. http://dx.doi.org/10.1038/nature01283

de Boer, J., A. Williams, G. Skavdis, N. Harker, M. Coles, M. Tolaini, T. Norton, K. Williams, K. Roderick, A.J. Potocnik, and D. Kioussis. 2003.

Transgenic mice with hematopoietic and lymphoid specific expression of Cre. *Eur. J. Immunol.* 33:314–325. http://dx.doi.org/10.1002/immu.200310005

Denning, M.F., A.A. Dlugosz, D.W. Threadgill, T. Magnuson, and S.H. Yuspa. 1996. Activation of the epidermal growth factor receptor signal transduction pathway stimulates tyrosine phosphorylation of protein kinase C delta. *J. Biol. Chem.* 271:5325–5331. http://dx.doi.org/10.1074/jbc.271.10.5325

Dinarello, C.A. 2009. Immunological and inflammatory functions of the interleukin-1 family. *Annu. Rev. Immunol.* 27:519–550. http://dx.doi.org/10.1146/annurev.immunol.021908.132612

Dlugosz, A.A., and S.H. Yuspa. 1993. Coordinate changes in gene expression which mark the spinous to granular cell transition in epidermis are regulated by protein kinase C. *J. Cell Biol.* 120:217–225. http://dx.doi.org/10.1083/jcb.120.1.217

Dlugosz, A.A., C. Cheng, E.K. Williams, A.G. Dharia, M.F. Denning, and S.H. Yuspa. 1994. Alterations in murine keratinocyte differentiation induced by activated rasHa genes are mediated by protein kinase C-alpha. *Cancer Res.* 54:6413–6420.

Dlugosz, A.A., C. Cheng, E.K. Williams, N. Darwiche, P.J. Dempsey, B. Mann, A.R. Dunn, R.J. Coffey Jr., and S.H. Yuspa. 1995. Autocrine transforming growth factor alpha is dispensible for v-rasHa-induced epidermal neoplasia: potential involvement of alternate epidermal growth factor receptor ligands. *Cancer Res.* 55:1883–1893.

Dlugosz, A.A., L. Hansen, C. Cheng, N. Alexander, M.F. Denning, D.W. Threadgill, T. Magnuson, R.J. Coffey Jr., and S.H. Yuspa. 1997. Targeted disruption of the epidermal growth factor receptor impairs growth of squamous papillomas expressing the v-ras(Ha) oncogene but does not block in vitro keratinocyte responses to oncogenic ras. *Cancer Res.* 57:3180–3188.

Dlugosz, A., G. Merlino, and S.H. Yuspa. 2002. Progress in cutaneous cancer research. *J. Investig. Dermatol. Symp. Proc.* 7:17–26. http://dx.doi.org/10.1046/j.1523-1747.2002.19631.x

Ehrenreiter, K., F. Kern, V. Velamoor, K. Meissl, G. Galabova-Kovacs, M. Sibilia, and M. Baccarini. 2009. Raf-1 addiction in Ras-induced skin carcinogenesis. *Cancer Cell.* 16:149–160. http://dx.doi.org/10.1016/j.ccr.2009.06.008

Elaraj, D.M., D.M. Weinreich, S. Varghese, M. Puhlmann, S.M. Hewitt, N.M. Carroll, E.D. Feldman, E.M. Turner, and H.R. Alexander. 2006. The role of interleukin 1 in growth and metastasis of human cancer xenografts. *Clin. Cancer Res.* 12:1088–1096. http://dx.doi.org/10.1158/1078-0432.CCR-05-1603

Ernst, M.K., L.L. Dunn, and N.R. Rice. 1995. The PEST-like sequence of I kappa B alpha is responsible for inhibition of DNA binding but not for cytoplasmic retention of c-Rel or RelA homodimers. *Mol. Cell. Biol.* 15:872–882.

Feldmeyer, L., M. Keller, G. Niklaus, D. Hohl, S. Werner, and H.D. Beer. 2007. The inflammasome mediates UVB-induced activation and secretion of interleukin-1beta by keratinocytes. *Curr. Biol.* 17:1140–1145. http://dx.doi.org/10.1016/j.cub.2007.05.074

González-García, A., C.A. Pritchard, H.F. Paterson, G. Mavria, G. Stamp, and C.J. Marshall. 2005. RalGDS is required for tumor formation in a model of skin carcinogenesis. *Cancer Cell.* 7:219–226. http://dx.doi.org/10.1016/j.ccr.2005.01.029

Gupta, S., A.R. Ramjaun, P. Haiko, Y. Wang, P.H. Warne, B. Nicke, E. Nye, G. Stamp, K. Alitalo, and J. Downward. 2007. Binding of ras to phosphoinositide 3-kinase p110alpha is required for ras-driven tumorigenesis in mice. *Cell.* 129:957–968. http://dx.doi.org/10.1016/j.cell.2007.03.051

Horton, L.W., Y. Yu, S. Zaja-Milatovic, R.M. Strieter, and A. Richmond. 2007. Opposing roles of murine duffy antigen receptor for chemokine and murine CXC chemokine receptor-2 receptors in murine melanoma tumor growth. *Cancer Res.* 67:9791–9799. http://dx.doi.org/10.1158/0008-5472.CAN-07-0246

Huitfeldt, H.S., A. Heyden, O.P.F. Clausen, E.V. Thrane, D. Roop, and S.H. Yuspa. 1991. Altered regulation of growth and expression of differentiation-associated keratins in benign mouse skin tumors. *Carcinogenesis.* 12:2063–2067. http://dx.doi.org/10.1093/carcin/12.11.2063

Joseloff, E., C. Cataisson, H. Aamodt, H. Ocheni, P. Blumberg, A.J. Kraker, and S.H. Yuspa. 2002. Src family kinases phosphorylate protein kinase C delta on tyrosine residues and modify the neoplastic phenotype of skin keratinocytes. *J. Biol. Chem.* 277:12318–12323. http://dx.doi.org/10.1074/jbc.M111618200

Keane, M.P., J.A. Belperio, Y.Y. Xue, M.D. Burdick, and R.M. Strieter. 2004. Depletion of CXCR2 inhibits tumor growth and angiogenesis in a murine model of lung cancer. *J. Immunol.* 172:2853–2860.

Khavari, P.A. 2006. Modelling cancer in human skin tissue. *Nat. Rev. Cancer.* 6:270–280. http://dx.doi.org/10.1038/nrc1838

Kleinridders, A., D. Schenten, A.C. Könner, B.F. Belgardt, J. Mauer, T. Okamura, F.T. Wunderlich, R. Medzhitov, and J.C. Brüning. 2009. MyD88 signaling in the CNS is required for development of fatty acid-induced leptin resistance and diet-induced obesity. *Cell Metab.* 10:249–259. http://dx.doi.org/10.1016/j.cmet.2009.08.013

Kupper, T.S., D.W. Ballard, A.O. Chua, J.S. McGuire, P.M. Flood, M.C. Horowitz, R. Langdon, L. Lightfoot, and U. Gubler. 1986. Human keratinocytes contain mRNA indistinguishable from monocyte interleukin 1 alpha and beta mRNA. Keratinocyte epidermal cell-derived thymocyte-activating factor is identical to interleukin 1. *J. Exp. Med.* 164:2095–2100. http://dx.doi.org/10.1084/jem.164.6.2095

Lee, W.Y., S.M. Fischer, A.P. Butler, and M.F. Locniskar. 1993. Modulation of interleukin-1 alpha mRNA expression in mouse epidermis by tumor promoters and antagonists. *Mol. Carcinog.* 7:26–35. http://dx.doi.org/10.1002/mc.2940070106

Lee, W.Y., M.F. Lockniskar, and S.M. Fischer. 1994. Interleukin-1 alpha mediates phorbol ester-induced inflammation and epidermal hyperplasia. *FASEB J.* 8:1081–1087.

Leng, X., T. Ding, H. Lin, Y. Wang, L. Hu, J. Hu, B. Feig, W. Zhang, L. Pusztai, W.F. Symmans, et al. 2009. Inhibition of lipocalin 2 impairs breast tumorigenesis and metastasis. *Cancer Res.* 69:8579–8584. http://dx.doi.org/10.1158/0008-5472.CAN-09-1934

Lichti, U., J. Anders, and S.H. Yuspa. 2008. Isolation and short-term culture of primary keratinocytes, hair follicle populations and dermal cells from newborn mice and keratinocytes from adult mice for in vitro analysis and for grafting to immunodeficient mice. *Nat. Protoc.* 3:799–810. http://dx.doi.org/10.1038/nprot.2008.50

Liss, C., M.J. Fekete, R. Hasina, C.D. Lam, and M.W. Lingen. 2001. Paracrine angiogenic loop between head-and-neck squamous-cell carcinomas and macrophages. *Int. J. Cancer.* 93:781–785. http://dx.doi.org/10.1002/ijc.1407

Loercher, A., T.L. Lee, J.L. Ricker, A. Howard, J. Geoghegen, Z. Chen, J.B. Sunwoo, R. Sitcheran, E.Y. Chuang, J.B. Mitchell, et al. 2004. Nuclear factor-kappaB is an important modulator of the altered gene expression profile and malignant phenotype in squamous cell carcinoma. *Cancer Res.* 64:6511–6523. http://dx.doi.org/10.1158/0008-5472.CAN-04-0852

Loukinova, E., G. Dong, I. Enamorado-Ayalya, G.R. Thomas, Z. Chen, H. Schreiber, and C. Van Waes. 2000. Growth regulated oncogene-alpha expression by murine squamous cell carcinoma promotes tumor growth, metastasis, leukocyte infiltration and angiogenesis by a host CXC receptor-2 dependent mechanism. *Oncogene.* 19:3477–3486. http://dx.doi.org/10.1038/sj.onc.1203687

Mittal, D., F. Saccheri, E. Vénéreau, T. Pusterla, M.E. Bianchi, and M. Rescigno. 2010. TLR4-mediated skin carcinogenesis is dependent on immune and radioresistant cells. *EMBO J.* 29:2242–2252. http://dx.doi.org/10.1038/emboj.2010.94

Miyazaki, H., V. Patel, H. Wang, R.K. Edmunds, J.S. Gutkind, and W.A. Yeudall. 2006. Down-regulation of CXCL5 inhibits squamous carcinogenesis. *Cancer Res.* 66:4279–4284. http://dx.doi.org/10.1158/0008-5472.CAN-05-4398

Moore, R.J., D.M. Owens, G. Stamp, C. Arnott, F. Burke, N. East, H. Holdsworth, L. Turner, B. Rollins, M. Pasparakis, et al. 1999. Mice deficient in tumor necrosis factor-alpha are resistant to skin carcinogenesis. *Nat. Med.* 5:828–831. http://dx.doi.org/10.1038/10552

Mueller, M.M. 2006. Inflammation in epithelial skin tumours: old stories and new ideas. *Eur. J. Cancer.* 42:735–744. http://dx.doi.org/10.1016/j.ejca.2006.01.014

Nakao, S., T. Kuwano, C. Tsutsumi-Miyahara, S. Ueda, Y.N. Kimura, S. Hamano, K.H. Sonoda, Y. Saijo, T. Nukiwa, R.M. Strieter, et al. 2005. Infiltration of COX-2-expressing macrophages is a prerequisite for IL-1 beta-induced neovascularization and tumor growth. *J. Clin. Invest.* 115: 2979–2991. http://dx.doi.org/10.1172/JCI23298

Naugler, W.E., and M. Karin. 2008. NF-kappaB and cancer-identifying targets and mechanisms. *Curr. Opin. Genet. Dev.* 18:19–26. http://dx.doi.org/10.1016/j.gde.2008.01.020

Ngo, V.N., R.M. Young, R. Schmitz, S. Jhavar, W. Xiao, K.H. Lim, H. Kohlhammer, W. Xu, Y. Yang, H. Zhao, et al. 2011. Oncogenically active MYD88 mutations in human lymphoma. *Nature.* 470:115–119. http://dx.doi.org/10.1038/nature09671

O'Hayer, K.M., D.C. Brady, and C.M. Counter. 2009. ELR+ CXC chemokines and oncogenic Ras-mediated tumorigenesis. *Carcinogenesis.* 30:1841–1847. http://dx.doi.org/10.1093/carcin/bgp198

Obermueller, E., S. Vosseler, N.E. Fusenig, and M.M. Mueller. 2004. Cooperative autocrine and paracrine functions of granulocyte colony-stimulating factor and granulocyte-macrophage colony-stimulating factor in the progression of skin carcinoma cells. *Cancer Res.* 64:7801–7812. http://dx.doi.org/10.1158/0008-5472.CAN-03-3301

Pierceall, W.E., L.H. Goldberg, M.A. Tainsky, T. Mukhopadhyay, and H.N. Ananthaswamy. 1991. Ras gene mutation and amplification in human nonmelanoma skin cancers. *Mol. Carcinog.* 4:196–202. http://dx.doi.org/10.1002/mc.2940040306

Porta, C., P. Larghi, M. Rimoldi, M.G. Totaro, P. Allavena, A. Mantovani, and A. Sica. 2009. Cellular and molecular pathways linking inflammation and cancer. *Immunobiology.* 214:761–777. http://dx.doi.org/10.1016/j.imbio.2009.06.014

Pylayeva-Gupta, Y., E. Grabocka, and D. Bar-Sagi. 2011. RAS oncogenes: weaving a tumorigenic web. *Nat. Rev. Cancer.* 11:761–774. http://dx.doi.org/10.1038/nrc3106

Ramirez, A., A. Page, A. Gandarillas, J. Zanet, S. Pibre, M. Vidal, L. Tusell, A. Genesca, D.A. Whitaker, D.W. Melton, and J.L. Jorcano. 2004. A keratin K5Cre transgenic line appropriate for tissue-specific or generalized Cre-mediated recombination. *Genesis.* 39:52–57. http://dx.doi.org/10.1002/gene.20025

Rice, N.R., and M.K. Ernst. 1993. In vivo control of NF-kappa B activation by I kappa B alpha. *EMBO J.* 12:4685–4695.

Roop, D.R., D.R. Lowy, P.E. Tambourin, J. Strickland, J.R. Harper, M. Balaschak, E.F. Spangler, and S.H. Yuspa. 1986. An activated Harvey ras oncogene produces benign tumours on mouse epidermal tissue. *Nature.* 323:822–824. http://dx.doi.org/10.1038/323822a0

Roop, D.R., H. Huitfeldt, A. Kilkenny, and S.H. Yuspa. 1987. Regulated expression of differentiation-associated keratins in cultured epidermal cells detected by monospecific antibodies to unique peptides of mouse epidermal keratins. *Differentiation.* 35:143–150. http://dx.doi.org/10.1111/j.1432-0436.1987.tb00162.x

Rundhaug, J.E., and S.M. Fischer. 2010. Molecular mechanisms of mouse skin tumor promotion. *Cancers (Basel).* 2:436–482.

Saijo, Y., M. Tanaka, M. Miki, K. Usui, T. Suzuki, M. Maemondo, X. Hong, R. Tazawa, T. Kikuchi, K. Matsushima, and T. Nukiwa. 2002. Proinflammatory cytokine IL-1 beta promotes tumor growth of Lewis lung carcinoma by induction of angiogenic factors: in vivo analysis of tumor-stromal interaction. *J. Immunol.* 169:469–475.

Sakurai, T., G. He, A. Matsuzawa, G.Y. Yu, S. Maeda, G. Hardiman, and M. Karin. 2008. Hepatocyte necrosis induced by oxidative stress and IL-1 alpha release mediate carcinogen-induced compensatory proliferation and liver tumorigenesis. *Cancer Cell.* 14:156–165. http://dx.doi.org/10.1016/j.ccr.2008.06.016

Schubbert, S., K. Shannon, and G. Bollag. 2007. Hyperactive Ras in developmental disorders and cancer. *Nat. Rev. Cancer.* 7:295–308. http://dx.doi.org/10.1038/nrc2109

Sparmann, A., and D. Bar-Sagi. 2004. Ras-induced interleukin-8 expression plays a critical role in tumor growth and angiogenesis. *Cancer Cell.* 6:447–458. http://dx.doi.org/10.1016/j.ccr.2004.09.028

Spencer, J.M., S.M. Kahn, W. Jiang, V.A. DeLeo, and I.B. Weinstein. 1995. Activated ras genes occur in human actinic keratoses, premalignant precursors to squamous cell carcinomas. *Arch. Dermatol.* 131:796–800. http://dx.doi.org/10.1001/archderm.1995.01690190048009

Streicher, K.L., N.E. Willmarth, J. Garcia, J.L. Boerner, T.G. Dewey, and S.P. Ethier. 2007. Activation of a nuclear factor kappaB/interleukin-1 positive feedback loop by amphiregulin in human breast cancer cells. *Mol. Cancer Res.* 5:847–861. http://dx.doi.org/10.1158/1541-7786.MCR-06-0427

Sundberg, J.P., A.A. Erickson, D.R. Roop, and R.L. Binder. 1994. Ornithine decarboxylase expression in cutaneous papillomas in SENCAR mice is associated with altered expression of keratins 1 and 10. *Cancer Res.* 54:1344–1351.

Swann, J.B., M.D. Vesely, A. Silva, J. Sharkey, S. Akira, R.D. Schreiber, and M.J. Smyth. 2008. Demonstration of inflammation-induced cancer and cancer immunoediting during primary tumorigenesis. *Proc. Natl. Acad. Sci. USA.* 105:652–656. http://dx.doi.org/10.1073/pnas.0708594105

Threadgill, D.W., A.A. Dlugosz, L.A. Hansen, T. Tennenbaum, U. Lichti, D. Yee, C. LaMantia, T. Mourton, K. Herrup, R.C. Harris, et al. 1995. Targeted disruption of mouse EGF receptor: effect of genetic background on mutant phenotype. *Science.* 269:230–234. http://dx.doi.org/10.1126/science.7618084

Tusher, V.G., R. Tibshirani, and G. Chu. 2001. Significance analysis of microarrays applied to the ionizing radiation response. *Proc. Natl. Acad. Sci. USA.* 98:5116–5121. http://dx.doi.org/10.1073/pnas.091062498

Van Waes, C. 2007. Nuclear factor-kappaB in development, prevention, and therapy of cancer. *Clin. Cancer Res.* 13:1076–1082. http://dx.doi.org/10.1158/1078-0432.CCR-06-2221

Vigne, S., G. Palmer, C. Lamacchia, P. Martin, D. Talabot-Ayer, E. Rodriguez, F. Ronchi, F. Sallusto, H. Dinh, J.E. Sims, and C. Gabay. 2011. IL-36R ligands are potent regulators of dendritic and T cells. *Blood.* 118:5813–5823. http://dx.doi.org/10.1182/blood-2011-05-356873

Wang, D., H. Wang, J. Brown, T. Daikoku, W. Ning, Q. Shi, A. Richmond, R. Strieter, S.K. Dey, and R.N. DuBois. 2006. CXCL1 induced by prostaglandin E_2 promotes angiogenesis in colorectal cancer. *J. Exp. Med.* 203:941–951. http://dx.doi.org/10.1084/jem.20052124

Whiteside, S.T., J.C. Epinat, N.R. Rice, and A. Israël. 1997. I kappa B epsilon, a novel member of the I kappa B family, controls RelA and cRel NF-kappa B activity. *EMBO J.* 16:1413–1426. http://dx.doi.org/10.1093/emboj/16.6.1413

Wislez, M., N. Fujimoto, J.G. Izzo, A.E. Hanna, D.D. Cody, R.R. Langley, H. Tang, M.D. Burdick, M. Sato, J.D. Minna, et al. 2006. High expression of ligands for chemokine receptor CXCR2 in alveolar epithelial neoplasia induced by oncogenic kras. *Cancer Res.* 66:4198–4207. http://dx.doi.org/10.1158/0008-5472.CAN-05-3842

Yeudall, W.A., and H. Miyazaki. 2007. Chemokines and squamous cancer of the head and neck: targets for therapeutic intervention? *Expert Rev. Anticancer Ther.* 7:351–360. http://dx.doi.org/10.1586/14737140.7.3.351

Yi, M., J.D. Horton, J.C. Cohen, H.H. Hobbs, and R.M. Stephens. 2006. WholePathwayScope: a comprehensive pathway-based analysis tool for high-throughput data. *BMC Bioinformatics.* 7:30. http://dx.doi.org/10.1186/1471-2105-7-30

Yi, M., U. Mudunuri, A. Che, and R.M. Stephens. 2009. Seeking unique and common biological themes in multiple gene lists or datasets: pathway pattern extraction pipeline for pathway-level comparative analysis. *BMC Bioinformatics.* 10:200. http://dx.doi.org/10.1186/1471-2105-10-200